

Os isotope systematics in Fogo Island: Evidence for lower continental crust fragments under the Cape Verde Southern Islands

Stéphane Escrig^{a,*}, Régis Doucelance^{b,c}, Manuel Moreira^a, Claude Jean Allègre^a

^aLaboratoire de Géochimie et Cosmochimie (UMR 7579 CNRS), Institut de Physique du Globe de Paris, Université Denis Diderot (Paris 7), 4 place Jussieu, 75252 Paris Cedex 05, France

^bGEOTOP-UQAM-McGILL, Case postale 8888, Succursale Centre-ville, Montréal, Canada, Qc H3C 3P8

^cNow at Laboratoire 'Magma et Volcans', Université Blaise-Pascal, CNRS (UMR 6524), Observatoire de Physique du Globe de Clermont-Ferrand, 5 rue Kessler, 63038 Clermont-Ferrand Cedex, France

Received 17 June 2004; received in revised form 8 February 2005; accepted 15 February 2005

Abstract

Os and Nd isotopic ratios as well as major and trace element compositions have been measured in 17 mafic lavas from Fogo Island, Cape Verde. These new data complement a previous archipelago-scale study (Southern and Northern Islands) by Doucelance et al. [Doucelance, R., Escrig, S., Moreira, M., Gariépy, C., Kurz, M., 2003. Pb-Sr-He isotope and trace element geochemistry of the Cape Verde Archipelago. *Geochim. Cosmochim. Acta*, 67 (19), 3717-3733], in which major, trace element contents and Sr-Pb-He isotopic compositions of lavas were determined. We also report Os-Sr-Nd-Pb isotopic ratios of 2 carbonatites from Fogo.

Fogo mafic lavas have Os-Sr-Nd-Pb isotopic ratios that define correlations similar to those previously observed for the Cape Verde Southern Islands and interpreted to reflect a mixture between a moderate HIMU end-member ($^{206}\text{Pb}/^{204}\text{Pb} \sim 20$), common to the Northern and Southern Islands of the archipelago, and an EM1-like end-member. Similar isotopic correlations are observed within the different lava flows which requires that the two end-members are mixed during the lava differentiation at shallow depth. The increasing contribution of the enriched end-member through time in Fogo lavas confirms the shallow origin for the EM1 signature.

As with Pb, Sr and He, the Os and Nd isotopic compositions of the moderate HIMU end-member are explained by the mixing of 1.6 Ga recycled oceanic crust (ROC) and lower mantle material (LM) and interpreted to represent the Cape Verde mantle plume expression. For the EM1-like end-member, the high $^{187}\text{Os}/^{188}\text{Os}$ ratios that are measured in mafic lavas preclude the sub-continental lithospheric mantle from being its origin, as previously proposed based on trace element and Pb, Sr and Nd isotopic compositions. Our new isotopic and trace element data still indicate that the enriched component is

* Corresponding author. Department of Earth and Planetary Sciences, Harvard University, 20 Oxford Street, Cambridge, MA 02138, USA. Tel.: +1 617 496 6983.

E-mail address: escrig@eps.harvard.edu (S. Escrig).

related to continental lithospheric material incorporated in the oceanic lithosphere during the opening of the Atlantic Ocean but requires the involvement of lower continental crust fragments.

© 2005 Elsevier B.V. All rights reserved.

Keywords: Osmium; OIB; Cape Verde; Lower continental crust

1. Introduction

Systematic analysis of Sr–Nd–Pb isotopic compositions in oceanic island basalts (OIB) and mid-oceanic ridge basalts (MORB) has led to the identification of several mantle end-members with extreme locations in isotopic diagrams (Allègre and Turcotte, 1985; White, 1985; Zindler and Hart, 1986; Allègre et al., 1986/87) and termed DMM (‘Depleted MORB Mantle’), HIMU (‘high $^{238}\text{U}/^{204}\text{Pb}$ ’), EM1 and EM2 (‘Enriched Mantle 1 and 2’) by Zindler and Hart (1986). However, most of the oceanic islands have intermediate positions in the Sr–Nd–Pb isotopic diagrams, which suggest end-members having similar characteristics but less extreme isotopic compositions. The differences in end-member isotopic compositions are currently debated. For example, while the extreme HIMU end-member is generally associated with old (~2 Ga) and altered recycled oceanic crust, the moderate HIMU-like signature can be explained by the mixing of this old oceanic crust with another mantle component and also by the recycling of relatively younger oceanic crust (‘young HIMU’, cf. Thirlwall (1997)). In the same way, the EM1-like signature can have different origins such as intramantle metasomatism processes (Hart, 1988; Hawkesworth et al., 1990), recycling of sediments associated with ancient oceanic crust (Weaver, 1991; Chauvel et al., 1992) or sub-continental lithospheric mantle (Cohen and O’Nions, 1982; McKenzie and O’Nions, 1983). Lastly, it has to be noted that noble gas results, notably high $^3\text{He}/^4\text{He}$ ratios measured in some oceanic island basalts, provide arguments in favour of another mantle component: a relatively undegassed reservoir thought to be the lower mantle (LM) (Kurz et al., 1982).

The Re/Os isotopic system provides new information on the nature and the composition of mantle end-members. Re and Os are both highly siderophile and chalcophile and have been strongly depleted in the

silicate Earth during the core formation. However, the upper mantle appears to have a broadly chondritic composition in such elements, supporting the model of a late veneer input during the Earth accretion (Allègre and Luck, 1980; Walker et al., 1996). During melting processes, Re behaves as a moderately incompatible element while Os is strongly compatible. Therefore, melting products such as crustal material have very high Re/Os relative to the residual mantle and rapidly develop high radiogenic $^{187}\text{Os}/^{188}\text{Os}$ by β^- decay of ^{187}Re to ^{187}Os ($\lambda = 1.666 \times 10^{-11} \text{ yr}^{-1}$, cf. Smoliar et al. (1996)). Furthermore, ancient sub-continental lithospheric mantle has been depleted in Re relative to Os by the crust extraction and has a lower than primitive upper mantle $^{187}\text{Os}/^{188}\text{Os}$ value (Meisel et al., 1996). Therefore, the $^{187}\text{Os}/^{188}\text{Os}$ ratio appears to be sensitive to the presence in basaltic sources either of important amounts of recycled crustal material, having high $^{187}\text{Os}/^{188}\text{Os}$ ratio but low Os concentration, or small amounts of sub-continental lithospheric mantle, having subchondritic $^{187}\text{Os}/^{188}\text{Os}$ ratio and mantle-like concentration.

Previous studies of the Cape Verde archipelago based on trace elements and isotopic measurements (Sr, Nd, Pb, U/Th, He ratios) have shown relatively clear variations between the Northern and Southern Islands. Lavas from the Southern Islands display trace elements and isotopic compositions that support the involvement of sub-continental lithospheric mantle (SCLM) in their source (Gerlach et al., 1988; Davies et al., 1989; Kokfelt et al., 1998). This result has motivated our Os study of Fogo Island where the current volcanism of the Cape Verde archipelago occurs. We report the first isotopic Os analyses as well as new major, trace element and $^{143}\text{Nd}/^{144}\text{Nd}$ measurements on samples previously analyzed for Pb, Sr and He isotopes by Doucelance et al. (2003).

The Os and Nd isotopic compositions confirm that Fogo lavas result from the mixture between a moderate HIMU end-member ($^{206}\text{Pb}/^{204}\text{Pb} \sim 20$) and

an EM1-like end-member, as previously proposed (Gerlach et al., 1988; Davies et al., 1989; Kokfelt et al., 1998). Together with the major and trace element compositions, the isotopic data suggests the contribution of the EM1-like end-member occurred during magma differentiation. The Os compositions of Fogo lavas combined with the other isotopic systems indicate this end-member is lower continental crust fragments, possibly with sub-continental lithospheric mantle, stored within the oceanic lithosphere during the opening of the Atlantic Ocean.

2. Geological Setting and sample location

The Cape Verde Islands are located in the central Atlantic between latitudes 15° and 17° N. The archipelago consists of ten major islands separated into the Southern Islands (Brava, Fogo, Santiago and Maio) and the Northern Islands (Santo Antão, São Vicente, Santa Luzia and São Nicolau), which also include the Eastern Islands (Boa Vista and Sal).

(Fig. 1). Summaries of the structure and geology of each island can be found in Matos Alves et al. (1979) and Gerlach et al. (1988).

Fogo Island is located in the southwest of the archipelago and forms the top of a large strato-volcano with a summit at 2829 m. A collapse caldera fills the northeast of the island and presently contains a more recent cone, inactive since the 18th century. Fogo is still a very active volcano with many smaller cones within the caldera associated with historic lava flows (1847, 1857, 1951, 1995) which erupted in the eastern part of the island (Day et al., 1999).

The 17 samples analyzed in this study were selected to span the whole volcanic series, from pre-caldera activity to the latest historic eruption in 1995. Samples F-01, -02, -18 and -20 are pre-caldera, coming from the western part of the island. F-11 and F-13, collected in the wall of the caldera, are syn- or post-caldera. Others (F-06, -07, -08, -10, -12, -14, -15, -16, -21, -22 and -24) are post-caldera and sample historic volcanism. Samples F-10 and -12 come from the 1785 lava flow, F-24 from the 1847, F-22 from the

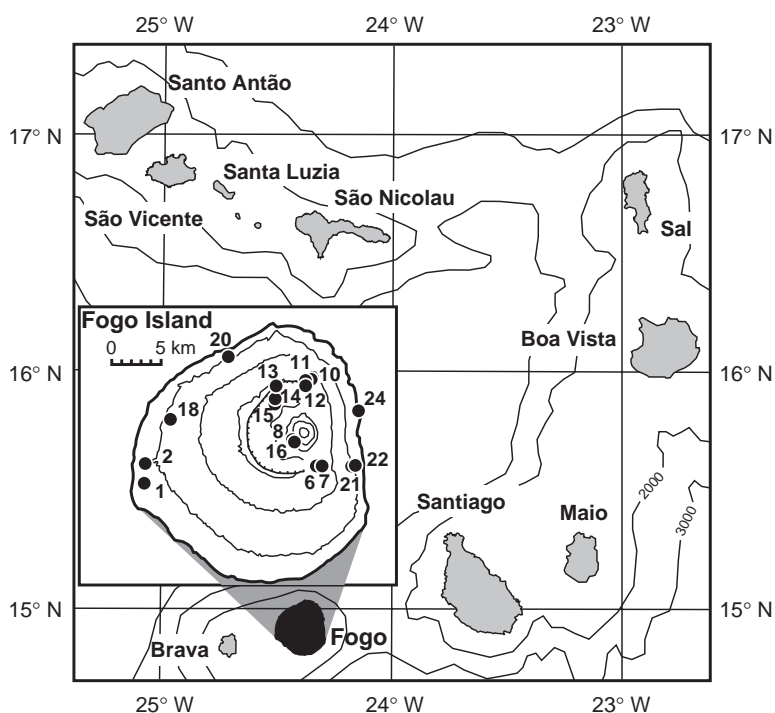


Fig. 1. Geographical location map and seafloor bathymetry of the Cape Verde archipelago including sampling map of Fogo modified after Doucelance et al. (2003).

1857, and F-06, -07 and -21 from the 1951, respectively. F-14 and -15 come from a separate lava flow also erupted in 1951. Lastly, F-08 and -16 sample the most recent volcanic activity of the island (1995). Sample locations are given in Table 2 and

shown in Fig. 1. The two carbonatites were collected in the western part of the island during a previous sampling campaign (Hodgson, 1986). NF 43 is a brown fine-grained carbonatite; NF 44 is mottled, with brown rhombs in a white/grey matrix.

Table 1

Major (wt.%) and trace element (ppm) concentrations of basalts from Fogo, Cape Verde

	F-01	F-02*	F-06	F-07*	F-08*	F-10	F-11	F-12	F-13	F-14	F-15*	F-16	F-18	F-20*	F-21	F-22	F-24*
SiO ₂	39.63	41.59	41.72	42.24	42.47	42.18	39.26	41.49	41.13	42.60	42.14	42.35	42.08	40.65	41.10	42.92	41.42
TiO ₂	4.39	4.07	3.83	3.74	3.80	3.73	3.64	3.77	4.01	3.67	3.65	3.83	3.07	4.40	4.01	3.34	3.53
Al ₂ O ₃	12.71	14.88	14.99	15.32	15.59	15.40	11.48	15.29	14.09	15.80	15.71	15.49	12.64	14.53	14.56	16.89	13.31
Fe ₂ O ₃	14.79	14.19	13.98	13.31	13.24	12.97	14.63	13.29	14.57	13.24	13.06	13.29	12.28	14.07	14.52	11.42	14.18
MgO	8.69	7.15	6.79	6.49	6.17	6.01	10.41	6.18	7.04	5.81	5.81	6.04	10.79	6.50	6.81	4.62	9.21
CaO	14.18	11.07	12.06	12.02	11.94	11.98	14.39	11.60	13.22	11.48	11.60	11.87	12.67	12.81	13.21	10.61	12.81
Na ₂ O	2.86	4.41	3.55	3.75	3.89	4.35	3.01	4.31	3.34	3.98	4.00	3.83	3.62	3.61	3.44	5.33	3.08
K ₂ O	1.75	2.18	2.47	2.60	2.74	2.88	0.39	2.89	1.86	2.75	2.77	2.69	1.96	2.39	2.28	3.50	1.92
MnO	0.19	0.18	0.19	0.20	0.20	0.21	0.19	0.21	0.20	0.20	0.21	0.20	0.20	0.20	0.21	0.22	0.20
P ₂ O ₅	0.59	0.60	0.83	0.82	0.84	0.91	0.77	0.87	0.64	0.89	0.91	0.81	0.71	0.70	0.79	0.95	0.74
Total	100.16	100.32	100.00	100.49	100.88	100.48	98.60	99.48	100.25	100.02	99.86	100.11	100.02	99.86	100.32	99.95	100.40
V	423	341	365	348	340	323	383	321	370	321	328	359	310	372	396.	291	350
Cr	129	144	112	94	62	58	477	63	74	54	55	58	627	66	89	12	350
Co	54.6	47.2	46.3	42.8	40.3	36.6	60.0	40.4	48.0	38.5	40.6	42.4	52.1	46.9	47.1	30.2	53.6
Ni	93.3	82.9	58.3	50.4	41.6	40.5	161.6	49.0	55.8	32.0	33.9	46.3	220	43.0	52.6	17.5	113
Cu	119	94	93	72	69	63	91	71	86	67	58	420	74	81	67	62	101
Zn	132	149	148	149	151	133	133	135	135	147	155	171	125	155	146	150	135
Ga	23.3	23.8	24.8	24.8	24.7	23.7	21.7	23.4	22.5	25.1	25.9	25.8	20.8	25.1	24.6	24.8	22.4
Rb	44.1	62.6	54.1	56.0	60.1	64.4	36.1	62.4	47.9	61.7	61.1	62.6	54.9	49.4	51.8	81.0	43.4
Sr	827	929	1000	1041	1066	1126	681	1092	906	1095	1104	1068	1089	1014	971	1350	893
Y	25.6	23.4	27.9	29.1	29.9	30.0	26.6	29.4	27.1	30.8	31.0	30.5	26.0	29.5	29.7	33.5	27.2
Zr	299	330	325	338	357	356	289	342	291	370	357	364	290	356	335	436	281
Nb	51.5	83.0	80.7	84.1	90.0	94.0	48.4	91.4	57.7	93.1	88.5	91.6	63.3	76.6	77.8	119	66.9
Cs	0.40	0.64	0.58	0.68	0.74	0.76	0.42	0.70	0.47	0.65	0.71	0.67	0.60	0.56	0.58	0.92	0.64
Ba	560	795	768	802	849	878	319	877	682	831	771	847	733	747	720	1036	634.0
La	37.0	44.9	46.9	56.2	59.4	63.0	43.4	61.1	45.7	62.1	56.8	61.4	59.2	48.5	46.9	76.1	46.9
Ce	95.1	97.6	116.1	124.0	131.0	132.0	110.0	130.1	112.1	133.0	124.0	131.2	120.3	110.0	117.4	155.9	100.0
Pr	12.3	11.6	14.4	14.8	15.7	16.1	13.9	15.8	13.9	16.5	15.4	15.9	14.2	14.0	14.9	18.7	13.1
Nd	51.3	46.5	57.5	57.1	62.6	63.7	57.2	62.5	56.2	66.1	63.5	63.8	56.5	58.2	59.7	71.7	54.4
Sm	10.53	9.09	11.00	10.80	11.40	12.17	11.00	11.74	11.04	12.58	11.30	12.10	10.46	10.80	11.49	13.02	9.97
Eu	3.26	2.84	3.48	3.41	3.70	3.73	3.44	3.65	3.43	3.98	3.64	3.80	3.22	3.70	3.66	4.02	3.25
Gd	8.47	6.74	8.95	8.78	9.06	6.05	8.60	9.22	8.58	9.60	9.41	9.61	7.96	8.78	9.10	10.18	8.18
Tb	1.13	0.98	1.20	1.22	1.33	1.26	1.16	1.26	1.16	1.31	1.25	1.25	1.10	1.25	1.25	1.39	1.09
Dy	5.76	5.00	6.22	6.12	6.49	6.61	6.09	6.68	6.03	6.77	6.33	6.67	5.64	6.47	6.57	7.15	5.70
Ho	0.94	0.87	1.01	1.02	1.03	1.10	0.96	1.07	1.00	1.14	1.12	1.10	0.93	1.06	1.09	1.23	0.97
Er	2.26	2.05	2.51	2.59	2.57	2.72	2.32	2.71	2.54	2.84	2.64	2.76	2.37	2.45	2.71	3.10	2.19
Tm	0.31	0.27	0.34	0.29	0.31	0.37	0.31	0.35	0.33	0.37	0.34	0.36	0.29	0.36	0.35	0.41	0.30
Yb	1.74	1.81	2.03	2.17	2.12	2.28	1.77	2.06	1.94	2.25	2.27	2.24	1.74	1.96	2.05	2.49	1.80
Lu	0.25	0.25	0.29	0.29	0.31	0.32	0.26	0.32	0.29	0.33	0.31	0.32	0.26	0.28	0.30	0.35	0.26
Hf	7.66	7.73	7.41	7.39	8.10	7.99	6.82	7.53	7.15	8.27	7.99	8.20	6.34	9.04	7.79	8.46	6.57
Ta	4.95	6.57	6.25	6.38	7.04	7.53	4.46	7.15	5.26	7.32	7.20	7.07	5.63	6.30	6.05	8.95	5.24
Pb	2.50	2.57	4.02	3.50	3.74	3.88	3.11	3.90	3.50	4.25	4.09	6.07	3.61	3.03	3.36	6.14	3.36
Th	3.02	4.47	4.23	5.11	5.73	5.39	3.41	5.24	4.31	4.84	5.62	5.07	4.86	4.06	4.06	6.47	4.01
U	0.76	0.97	1.01	1.05	1.19	1.32	1.09	1.27	1.09	1.16	1.25	1.18	1.57	0.96	1.01	1.61	0.88

* From Doucelance et al. (2003).

3. Analytical techniques

Osmium, rhenium and neodymium analyses were performed on whole rocks, using the same powder crushed into an agate mortar. Re–Os analyses were done on 2–3 g samples. Osmium chemical separations including extraction and purification steps are described in detail elsewhere (Birck et al., 1997). Osmium and rhenium isotopic ratios were measured as OsO_3^- and ReO_4^- oxides on a Finnigan Mat 262 using negative thermal ionization and single-collection on an Ion Counting Multiplier. Os blanks ($n=5$) were on the average: 0.036 ± 0.009 pg/g with $^{187}\text{Os}/^{188}\text{Os}=0.35 \pm 0.09$; Re blanks range from 1.3 to 2.3 pg/g (mean=1.7 pg/g). Blank correction for the Os isotopic ratio ranges from 0.05% to 0.42% (Table 2). Measured ratios were also corrected for oxygen. Within-run 2σ precisions vary between 0.46% and 3.63% for the $^{187}\text{Os}/^{188}\text{Os}$ ratio. These values are larger than the total external reproducibility of 0.13% that was obtained on Os IPGP internal standards. It is consistent with the low Os concentration of samples and the lower signal intensity during acquisition. Replicate analyses of the $^{187}\text{Os}/^{188}\text{Os}$ ratio agree within 0.3–0.8%. Due to the low Os content and to the heterogeneous distribution of Os inside samples, replicate measurements of Os concentration display expected variations ranging from 3.9% to 10.7%.

Neodymium analyses were done on the same dissolved fraction used by Doucelance et al. (2003) for Sr analyses. Nd chemical separation is based on the procedure described in Richard et al. (1976). Neodymium measurements were performed in static multi-collection mode on a Finnigan Triton and corrected for mass discrimination using $^{144}\text{Nd}/^{146}\text{Nd}=0.7219$. Lead and strontium analyses of carbonatites were performed following the procedure described for basalts in Doucelance et al. (2003).

Major and trace element compositions were measured by the “Service d’Analyses des Roches et des Minéraux” at CRPG/Nancy. Following alkaline melting with LiBO_2 and nitric acid dissolution, major abundances have been determined by ICP-AES with a precision better than 1% except for CaO , Na_2O , K_2O and MnO (<2%) and P_2O_5 (<10%). Trace element composition were determined by ICP-MS with a precision better than 5% for most elements except for Pb (<20%), Cr and Cs (<15%) Ni, Lu and Tm

(<10%), U (<8%), Dy and Th (<7%), Gd (6%) and Sr (<4%). Trace element data for international standards measured by the SARM are available on their web site (<http://www.crbg.cnrs-nancy.fr/SARM/>) and in Cari-gnan et al. (2001).

4. Results

4.1. Major and trace element compositions

Whole-rock analyses of major and trace elements are reported in Table 1. Using the alkali–silica nomenclature, Fogo lavas are mostly basanites, tephrites and nephelinites. In comparison to the other Cape Verde islands, Fogo lavas (Fig. 2) have relatively high Fe_2O_3 (11.42–14.79 wt.%) and TiO_2 (3.07–4.40 wt.%) and low MgO content (4.6–10.8 wt.%) for a similar range of SiO_2 contents (39.26–42.92 wt.%). The trace element compositions show homogenous primitive mantle-normalized trace element patterns, similar to those from previous studies (Gerlach et al., 1988; Davies et al., 1989; Doucelance et al., 2003) and from Tristan da Cunha basalts (Cliff et al., 1991). These results confirm the EMI-like signature of Fogo lavas with relative depletion in Pb, Th and U and large enrichments for Ba, Nb, La and Rb.

The osmium concentrations range from 2.2 to 28.6 ppt (Table 2 and Fig. 2), among the lowest Os content measured in OIB, particularly in Atlantic archipelagos like the Azores and the Canary Islands (Hauri and Hart, 1993; Reisberg et al., 1993; Marcantonio et al., 1995; Roy-Barman and Allègre, 1995; Bennet et al., 1996; Hauri et al., 1996; Widom and Shirey, 1996; Lassiter and Hauri, 1998; Brandon et al., 1999; Widom et al., 1999; Schiano et al., 2001; Eisele et al., 2002). The rhenium concentrations vary from 281 to 1826 ppt.

4.2. Isotopic compositions

Except sample F-22, which has the lowest Os content together with the most radiogenic Os isotopic ratio (0.1548), Fogo lavas define a small range from 0.1323 to 0.1369 (Fig. 3). Compared to this range, the uncertainty on $^{187}\text{Os}/^{188}\text{Os}$ ratios (from 0.46% to 3.63%) appear to be relatively large. Nevertheless, the

Table 2
Sample locations and Os, Sr, Nd and Pb isotopic compositions of Fogo basalts and carbonatites

Samples	Latitude E°	Longitude W°	Volc. unit	Re (ppt)	Os (ppt)	$^{187}\text{Re}/$ ^{188}Os	$(^{187}\text{Os}/$ $^{188}\text{Os})_m$	Blank correction (%)	$(^{187}\text{Os}/$ $^{188}\text{Os})_i$	$^{87}\text{Sr}/^{86}\text{Sr}$	$^{143}\text{Nd}/^{144}\text{Nd}$	$^{206}\text{Pb}/^{204}\text{Pb}$	$^{207}\text{Pb}/^{204}\text{Pb}$	$^{208}\text{Pb}/^{204}\text{Pb}$
<i>Basalts</i>														
F-01	14°54'00	24°30'00	Pre-caldera	674	18.30	176.5	0.1334 (23)	0.11		0.703685 (18)	0.512760 (4)	19.105 (8)	15.553 (9)	38.884 (31)
F-02	14°55'04	24°29'57	Pre-caldera	488	18.72	125.1	0.1343 (23)	0.29		0.703723 (23)	0.512727 (3)	19.064 (14)	15.567 (17)	38.880 (56)
F-18	14°57'28	24°28'32	Pre-caldera	444	18.21	117.1	0.1323 (06)	0.10		0.703546 (20)	0.512764 (3)	19.220 (8)	15.563 (9)	38.914 (31)
F-20	14°00'53	24°25'18	Pre-caldera	955	11.61	394.8	0.1343 (08)	0.07		0.703722 (22)	0.512735 (9)	19.062 (11)	15.548 (14)	38.822 (47)
F-20b	14°00'53	24°28'18	Pre-caldera		12.06		0.1343 (07)	0.07						
F-11	14°59'39	24°20'54	Caldera wall	281	28.60	47.1	0.1331 (09)	0.05		0.703665 (21)	0.512759 (3)	19.077 (11)	15.566 (9)	38.947 (44)
F-13	14°59'19	24°22'40	Caldera wall	620	7.13	417.6	0.1352 (08)	0.26		0.703715 (19)	0.512733 (9)	19.109 (8)	15.552 (9)	38.901 (31)
F-10	14°59'42	24°20'40	1785	729	15.28	228.8	0.1330 (18)	0.08		0.703616 (24)	0.512745 (4)	19.133(8)	15.560 (9)	38.917 (31)
F-12	14°59'39	24°20'54	1785	456	16.32	134	0.1347 (14)	0.07		0.703625 (20)	0.512758 (2)	19.143 (13)	15.577 (9)	38.975 (31)
F-24	14°57'56	24°17'38	1847	714	20.03	172	0.1334 (07)	0.40		0.703761 (18)	0.512728 (4)	18.969 (11)	15.562 (14)	38.804 (47)
F-24b	14°57'56	24°17'38	1847	553	18.90	141.1	0.1328 (09)	0.38						
F-22	14°55'15	24°17'40	1857	961	2.20	2116.3	0.1548 (56)	0.42		0.703656 (21)	0.512765 (3)	19.094 (8)	15.561 (9)	38.898 (31)
F-06	14°54'56	24°20'23	1951	1826	9.98	878	0.1362 (16)	0.12		0.703738 (20)	0.512726 (3)	18.900 (8)	15.539 (9)	38.731 (31)
F-07	14°54'56	24°20'23	1951	667	7.07	471.2	0.1360 (09)	0.09		0.703789 (19)	0.512722 (4)	18.882 (11)	15.530 (14)	38.701 (46)
F-07b	14°54'56	24°20'23	1951	543	6.79	368.7	0.1349 (12)	0.07						
F-14	14°58'41	24°22'42	1951	494	8.12	291.8	0.1348 (13)	0.14		0.703758 (22)	0.512725 (18)	18.935 (8)	15.549 (9)	38.772 (31)
F-15	14°58'23	24°22'42	1951	973	5.75	812.9	0.1356 (10)	0.10		0.703738 (22)	0.512728 (19)	18.930 (11)	15.551 (14)	38.790 (56)
F-15b	14°58'23	24°22'42	1951	868	6.45	645.9	0.1369 (17)	0.09						
F-21	14°55'13	24°17'41	1951	1085	8.09	643.3	0.1336 (20)	0.15		0.703727 (18)	0.512736 (2)	19.020 (8)	15.554 (9)	38.832 (31)
F-16	14°56'19	24°21'38	1995	1081	4.79	1083.5	0.1358 (17)	0.24		0.703764 (19)	0.512737 (4)	18.932 (8)	15.537 (9)	38.752 (31)
F-08	14°56'23	24°21'40	1995	707	4.40	768.9	0.1358 (09)	0.14		0.703734 (22)	0.512737 (5)	18.937 (11)	15.558 (9)	38.814 (44)
<i>Carbonatites</i>														
NF 43				1623	22.87	343.1	0.1924 (20)	0.16	0.1698 (39)	0.703156 (16)	0.512930 (6)	19.865 (8)	15.604 (9)	39.208 (31)
NF 44				481	12.60	184.4	0.1839 (24)	0.22	0.1718 (48)	0.703158 (20)	0.512926 (3)	19.866 (8)	15.597 (9)	39.189 (31)

Numbers in parentheses are 2σ errors referring to the last digits. Samples ending with “b” are Re–Os duplicates. Sr and Pb ratios are from Doucelance et al. (2003). Mean values have been used in case of Pb duplicate analyses. $^{187}\text{Os}/^{188}\text{Os}$ ratios of carbonatites are corrected for Re decay using a mean age of 4 Ma.

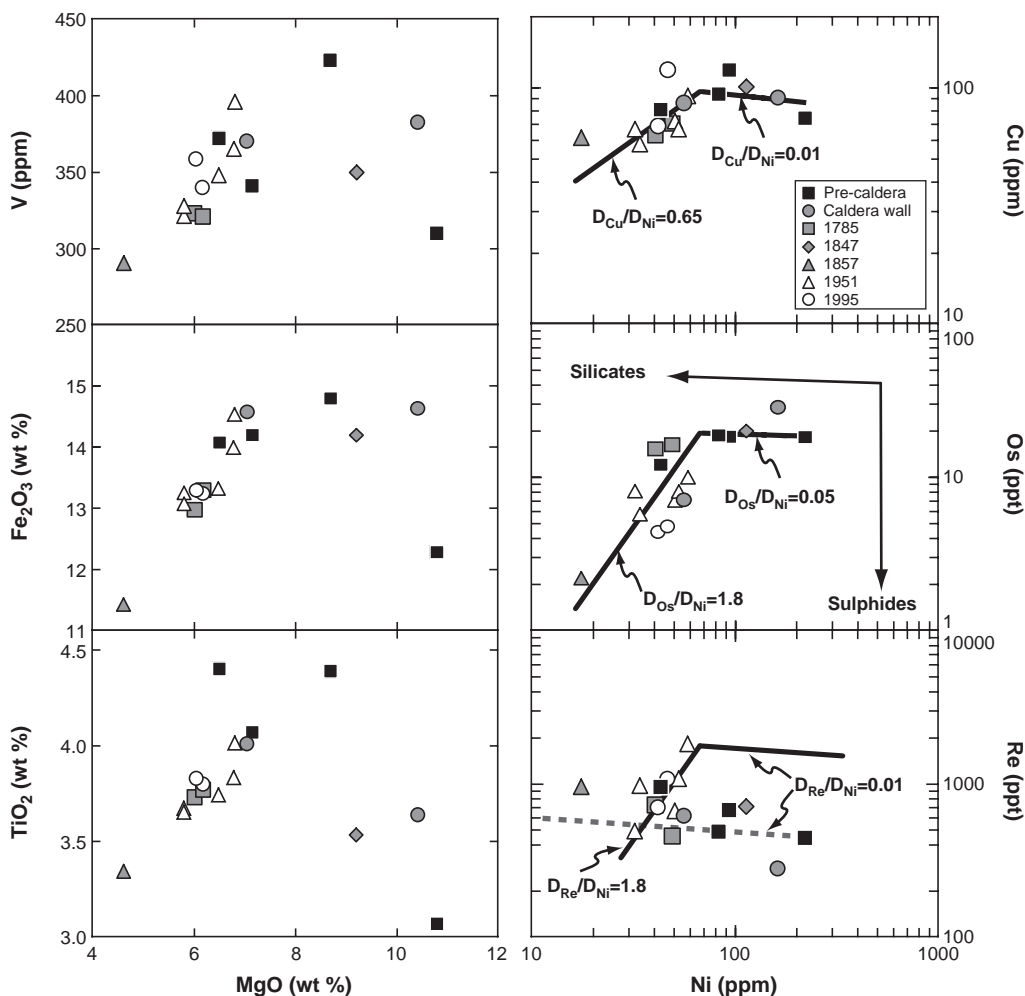


Fig. 2. Major and trace element variations of Fogo lavas. Though Fogo mafic lavas are not derived from a same parental magma, the Fe_2O_3 – TiO_2 – V – MgO variations suggest they have been differentiated first by crystallization of olivine and cpx and then by Fe–Ti oxide formation. The variations of Os and Cu versus Ni show that Fe–Ti oxide is a fractionating phase. Thick lines represent a fractional crystallization model starting from a primary melt with 220 ppm Ni, 18 ppt Os and 85 ppm Cu. The first step corresponds to an evolution with $D_{\text{Os}}/D_{\text{Ni}}=0.05$ and $D_{\text{Cu}}/D_{\text{Ni}}=0.01$. The second step begins at 65 ppm Ni with ratios of Os and Cu partition coefficients over that of Ni changed to $D_{\text{Os}}/D_{\text{Ni}}=1.8$ and $D_{\text{Cu}}/D_{\text{Ni}}=0.65$. The chalcophile property of Os and Cu supports that the change of their partition coefficients essentially reflects the formation of sulphides associated with Fe–Ti oxide formation. The overall negative trend in the Re vs. Ni diagram failed to be reproduced by a single-stage differentiation (dashed line) starting from the most primitive sample and a $D_{\text{Re}}/D_{\text{Ni}}$ as low as 0.01. The positive trend defined by the 1951–1995 lava flows can be reproduced by a two-step crystallisation model (thick line), starting at 220 ppm Ni and 1600 ppt Re with $D_{\text{Re}}/D_{\text{Ni}}=0.01$ and $D_{\text{Re}}/D_{\text{Ni}}=1.8$ below 65 ppm Ni, which support the chalcophile property of Re.

analytical scatter cannot account for all the variation observed and the overall positive trend with the inverse of ^{188}Os (Fig. 3). Global correlations with the other isotopic ratios (Fig. 4) support that the Os isotopic variation reflects the mixture between the two end-members previously identified. In addition, the correlations within flows between Os and Pb and Sr

isotopic composition despite the fact that the samples are indistinguishable within the quoted uncertainties also confirms that the isotopic variations observed are real.

Fogo lavas have neodymium isotopic ratios ranging from 0.512718 to 0.512765. These isotopic ratios are similar to those previously measured for Fogo,

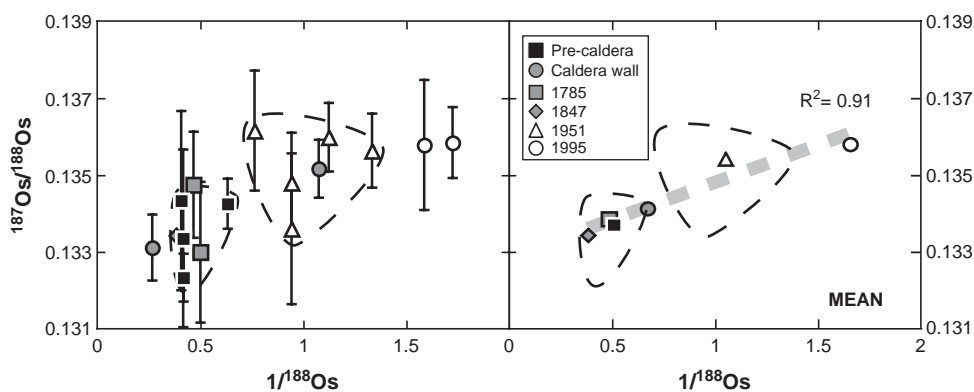


Fig. 3. $^{187}\text{Os}/^{188}\text{Os}$ – $1/^{188}\text{Os}$ variation for Fogo lavas. Sample F-22 from 1857, which has the lowest Os content as well as the highest $^{187}\text{Os}/^{188}\text{Os}$ ratio, plots outside the range represented. Taken as a whole, Fogo lavas define a global positive trend, feature accentuated by the use of the average compositions as shown by the dashed grey line ($r^2=0.91$), which suggests a binary mixing. At the lava flow scale, basalts from the 1951 lava flows and pre-caldera group, which represent the most sampled groups, do not define any positive trend, implying that the intra-lava flow isotopic heterogeneity has been produced prior to the end of the differentiation. The lack of intra-lava flow relationship and the correlation at the volcano scale imply that the contribution of the radiogenic Os end-member occur during the magma differentiation.

after correction of Nd isotope ratios from Gerlach et al. (1988) for inter-laboratory bias (see Hoernle et al. (2002) for details).

Os–Sr–Nd–Pb compositions are also reported for two carbonatites from Fogo (Table 2). NF43 and NF44 have more radiogenic $^{187}\text{Os}/^{188}\text{Os}$ (0.1924 and 0.1839, respectively) than mafic lavas for concentrations of the same order (22.9 and 12.6 ppt, respectively). These radiogenic Os compositions are in agreement with those measured in carbonatites from the Canary Islands (Widom et al., 1999). Earlier works found ages of 3.4 ± 1.0 Ma (Lancelot and Allègre, 1974) and 4 Ma (Hoernle et al., 2002) for the Fogo carbonatites. In a $^{187}\text{Os}/^{188}\text{Os}$ vs. $^{187}\text{Re}/^{188}\text{Os}$ diagram, the two samples we analyzed yield an age of 3.2 ± 1.2 Ma, consistent with those previously proposed. Nevertheless, having no evidence of a common history for our two samples, the mean age of 4 Ma proposed by Hoernle et al. (2002) is used, leading to corrected $^{187}\text{Os}/^{188}\text{Os}$ ratios of 0.1698 ± 0.039 and 0.1718 ± 0.048 for NF43 and NF44, respectively. NF43 and NF44 also have very similar Sr–Nd–Pb isotopic compositions, identical within the uncertainty. The two carbonatites fall within the restricted range of previous analyses of carbonatites from Fogo (Gerlach et al., 1988; Hoernle et al., 2002). Their signature is less radiogenic than basaltic lavas for Sr isotopes ($^{87}\text{Sr}/^{86}\text{Sr}=0.703158$), but more radiogenic for Nd ($^{143}\text{Nd}/^{144}\text{Nd}=0.512930$) and Pb isotopes

$$\left(\begin{array}{l} ^{206}\text{Pb}/^{204}\text{Pb} = 19.868; \quad ^{207}\text{Pb}/^{204}\text{Pb} = 15.599; \\ ^{208}\text{Pb}/^{204}\text{Pb} = 39.201. \end{array} \right)$$

4.3. Isotopic variability within lava flows

The mafic lavas we analyzed correspond to at least six different volcanic series with different ages of eruption. The distinction of the different groups reveals an important isotopic variability within each lava flow. The two groups with more than two samples (i.e., 1951 and pre-caldera groups) have Os, Pb, Sr and Nd isotopic ratios that define binary mixing trends (Fig. 4). The basalts from 1951 have particularly low mean Os contents (~ 7.8 ppt), making them highly sensitive to post-differentiation contamination by radiogenic material. However, the inverse of Os contents of these samples does not correlate with $^{187}\text{Os}/^{188}\text{Os}$, indicating that they have not been significantly contaminated after differentiation (Fig. 3). Instead, the almost constant values of differentiation index associated with the isotopic variation implies that the mixture occurred prior to the end of magma differentiation and that the isotopic heterogeneity is preserved within the magma.

Pre-caldera samples define a linear correlation in $^{187}\text{Os}/^{188}\text{Os}$ – $^{187}\text{Re}/^{188}\text{Os}$ diagram (not shown) that could represent either an isochron (395 ± 216 Ma and $(^{187}\text{Os}/^{188}\text{Os})_0=0.1317$) or a binary mixture. The mixture hypothesis is supported by the correla-

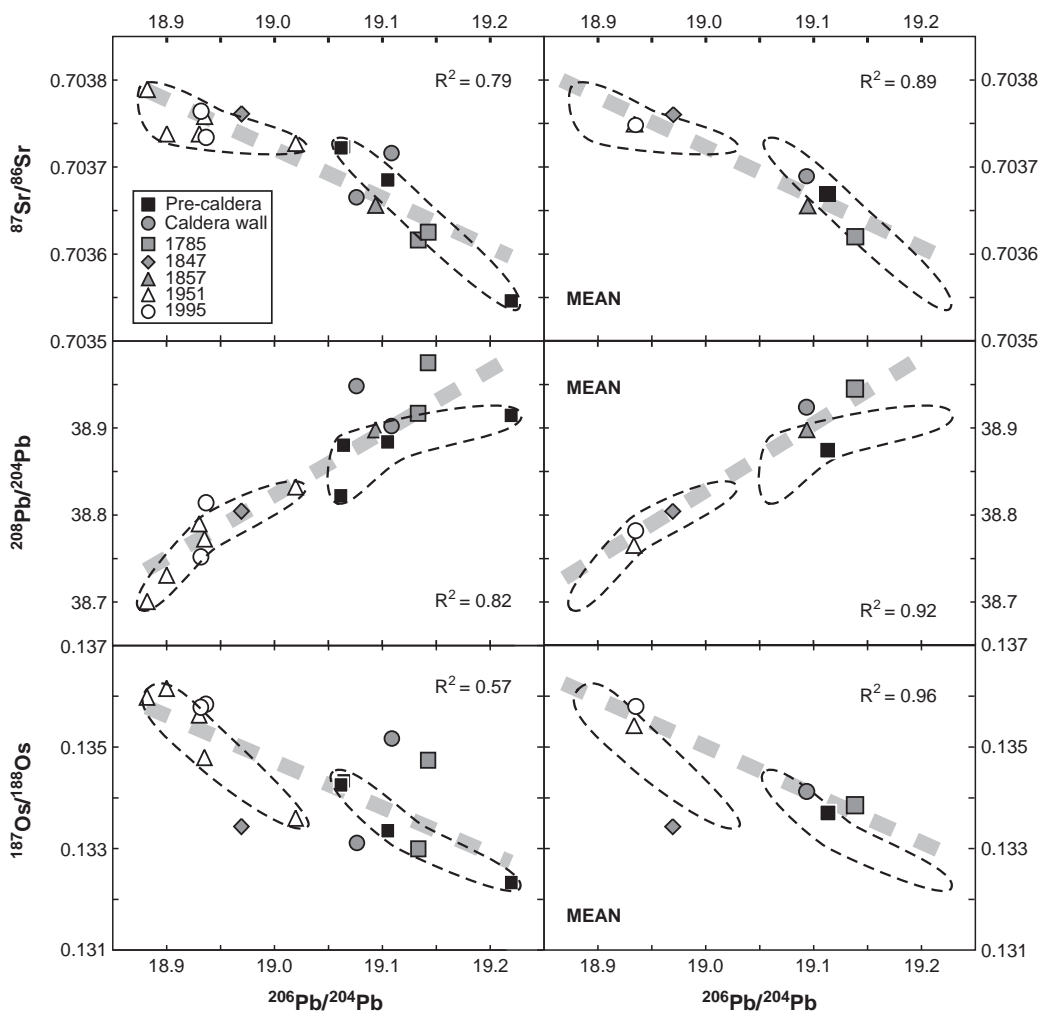


Fig. 4. $^{87}\text{Sr}/^{86}\text{Sr}$, $^{208}\text{Pb}/^{204}\text{Pb}$ and $^{187}\text{Os}/^{188}\text{Os}$ vs. $^{206}\text{Pb}/^{204}\text{Pb}$ variations of Fogo lavas. The 1951 lava flows and pre-caldera samples define trends in the isotopic diagrams (fields delimited by dashed lines) that are interpreted to reflect binary mixing. The entire dataset also defines correlations as shown by the thick dashed grey line, which represent the best-fit lines. Using the average isotopic compositions improves these correlations. Due to the $^{187}\text{Os}/^{188}\text{Os}$ scatter within a single lava flow, the best-fit curve in the $^{187}\text{Os}/^{188}\text{Os}$ vs. $^{206}\text{Pb}/^{204}\text{Pb}$ diagram is calculated using the lava flows which are sampled at least twice. The correlations defined by the average isotopic compositions are similar to the correlations within the 1951 and pre-caldera data, supporting a common origin for the intra-lava Os–Pb–Sr–Nd isotopic variations and the Fogo basalt isotopic evolution through time.

tions between the isotopic ratios and the incompatible element ratios such as Ba/Nb or Ba/La defined by the pre-caldera samples. Moreover, correlations between Sr–Nd–Pb isotopes indicate a binary mixture and, since the Os isotopes correlate with Sr–Nd–Pb, their variations should reflect the same mixture. Correcting Os isotopic compositions for post-eruption decay would reduce the Os variability within the pre-caldera group but would have no effect on the

other isotopic ratios and remove the pre-caldera samples from the overall Pb–Os and Sr–Os correlations (Fig. 4).

The isotopic compositions of samples from the groups with two samples (Caldera wall and 1785 lava flow) do not define linear trends parallel to those defined by 1951's lava flows and pre-caldera samples. Without a more numerous sampling, discussing the origin of their intra-lava isotopic variability remains

somewhat speculative. Except for Os isotopic composition of sample F-22, the other isotopic compositions are within the range defined by the most numerous groups.

4.4. Temporal isotopic variations

The trends defined by the 1951 and pre-caldera groups are similar to those defined by the whole dataset, suggesting they reflect the same mixture. In order to study the temporal evolution of Fogo volcanism, we consider here the average isotopic compositions of each lava flow. As reported in Fig. 4, the average isotopic compositions define correlations, similar to those defined by the whole dataset, which can be explained by a mixture in variable proportions of two end-members. Due to their similarities in major, trace element and isotopic compositions, mafic lavas from the 1951 and 1995 lava flows can be interpreted to be representative of the current volcanism. Pre-caldera samples display Os, Pb, Sr and Nd ratios distinct from those measured in samples from the 1951–1995 lava flows (Fig. 4).

Except for one pre-caldera sample, the 1785 lava flow display the largest HIMU signature measured in this study and plot within the pre-caldera field. The sample from the 1847 lava flow plot within the 1951–1995 lava flow fields while the sample from the 1857 lava flow plot in the pre-caldera field (see Fig. 4). While the Pb, Sr and Nd isotopic compositions of the 1847 and 1857 samples are consistent with the correlations defined in the isotopic diagrams, these two samples have Os isotopic ratios plotting outside of the correlations defined by the other lava flows. The Os isotopic ratio of sample F-24 (1847 lava flow) is within the range defined by the other lava flows, suggesting that the deviation is caused by a sampling bias. Concerning the 1857 lava flow, sample F-22 has the lowest Os content measured in this study together with a high $^{187}\text{Os}/^{188}\text{Os}$ ratio (0.1548) that strongly differs from the isotopic compositions measured in other Fogo lavas. This feature strongly suggests that its Os isotopic composition reflect a post-differentiation contamination by radiogenic material such as old oceanic crust forming the sea floor.

Due to the short time interval between the 1847 and 1857 eruptions and to the isotopic scatter existing

within the 1951 lava flow and the pre-caldera group, the two samples from the 1847 and 1857 lava flows could be grouped together. Such a grouping emphasizes the temporal isotopic evolution existing in the historic lava flows, starting from the moderate HIMU composition of the 1785 lava flow and pre-caldera group, toward the enriched composition (i.e. high $^{87}\text{Sr}/^{86}\text{Sr}$ and $^{187}\text{Os}/^{188}\text{Os}$ ratios and low $^{206}\text{Pb}/^{204}\text{Pb}$ and $^{143}\text{Nd}/^{144}\text{Nd}$ ratios) of the 1951–1995 lava flows, through the 1847 and 1857 lava flow compositions. A similar isotopic distinction has been previously observed in Fogo and Santiago basalts and interpreted as a temporal evolution of the proportions of the different end-members involved in the magmatic source (Gerlach et al., 1988).

5. Discussion

5.1. Re–Os behaviour during differentiation

Despite the fact that Fogo lavas belong to different lava series and derive from different parental magmas, their composition in major elements suggests that they have experienced similar episodes of differentiation. The evolution of the TiO_2 , Fe_2O_3 and V contents relative to MgO (Fig. 2) supports a differentiation by fractional crystallization that may occur first by crystallization of olivine and clinopyroxene and later by crystallization of Fe–Ti oxides. The evolution of Os content with MgO and Ni contents is comparable to TiO_2 evolution (Fig. 2), with a change of slope at $\text{MgO}=7.1$ wt.% and $\text{Ni}=65$ ppm. Since the silicates have very low Os content, the decrease in Os suggests the formation and fractionation of sulphides (Burton et al., 2002). The similar evolution of Os and Cu (Fig. 2), both chalcophile elements, confirms that the increase of slope is related to sulphide formation enhanced by Fe–Ti oxide precipitation that induces a marked sulphur oversaturation in the melt. The bulk partition coefficient for Os can be estimated relative to that of Ni for the two steps of crystallization. A fractional crystallization model reproducing the Ni–Os trends is reported in Fig. 2, starting from a hypothetical primary melt with 220 ppm Ni, 18 ppt Os and 85 ppm Cu and $D_{\text{Os}}/D_{\text{Ni}}=0.05$ and $D_{\text{Cu}}/D_{\text{Ni}}=0.01$. At 65 ppm Ni, the ratios of Os and Cu partition coefficients over that of Ni increase signifi-

cantly to $D_{\text{Os}}/D_{\text{Ni}}=1.8$ and $D_{\text{Cu}}/D_{\text{Ni}}=0.65$. The estimation of bulk partition coefficient for Os is difficult because D_{Ni} is changing during crystallization (Hart and Davis, 1978).

The high Re contents of Fogo lavas contrast with the low contents measured in Hawaiian subaerial lavas (<350 ppt), which have been attributed to reflect Re degassing during the eruption (Lassiter, 2003). Our dataset define an overall negative trend in the Re vs. Ni diagram which cannot be produced by a single-stage differentiation starting from the most primitive sample (Fig. 2). The positive trend defined by the 1951–1995 lava flows is similar to those defined in the other diagrams reported in Fig. 2, which suggests that sulphide formation has an significant effect on the evolution of Re content. Such a positive trend can be reproduced using a $D_{\text{Re}}/D_{\text{Ni}}$ equal to 1.8 for the second step of crystallization and the high Re content of F-06 requires a Re content up to 1600 ppt for the starting melt used for the first step. The dispersion of Fogo lavas in the Re vs. Ni diagram confirms that the different groups of samples identified above have to be derived from different parental magmas, with initial Re content as low as 150 and up to 1600 ppt for the recent lava flows. The high initial Re content required for the recent lava flows, which have the more enriched signature, suggests that the Re content is strongly influenced by the enriched component contribution. The initial Re content should be even higher if the magmas have encountered a significant degassing.

5.2. Origin of Fogo basalt isotopic variations

The correlations defined by the Os, Pb, Sr and Nd isotopic compositions of Fogo lavas support the existence of binary mixing between a moderate HIMU and an EM1-like end-member. The fact that these correlations are similar to the intra-lava flow trends defined by pre-caldera and 1951 groups (Fig. 4) suggests they reflect mixing of the same components. The existence of isotopic correlation within a single lava flow also implies that the mixture occurred after the magma formation and was not followed by an efficient homogenization.

The linear relationship observed between the mean $^{187}\text{Os}/^{188}\text{Os}$ and $1/^{188}\text{Os}$ ratios (Fig. 3) can be interpreted either as (1) the mixing of two end-

members, one with high $^{187}\text{Os}/^{188}\text{Os}$ and low Os content and one with low $^{187}\text{Os}/^{188}\text{Os}$ and high Os content, or as (2) the addition of radiogenic material during or after the magma differentiation, which has a greater effect on the low Os content lava. The first hypothesis would imply that the measured Os concentrations directly reflect the proportion of mixing of the two end-members involved and should not correlate with indices of fractionation. However, it has been shown above that the Os content variation of Fogo basalts is consistent with differentiation processes, supporting the second hypothesis. Within a given lava flow the Os isotopes do not correlate with differentiation indices. This suggests that the contribution of the Os radiogenic end-member occurred prior to the end of the magma differentiation, producing an isotopic heterogeneity that is preserved in the magma, while differentiation has obscured the initial Os concentration variations.

To summarize, the combination of the different scales of variation imply that the enriched signature of Southern Cape Verde Islands is related to a shallow contamination. The enriched end-member has to interact with the magma during its differentiation and affect the Os–Pb–Sr–Nd isotopic compositions. This contribution can correspond either to the addition of another silicate melt with distinct isotopic composition or to the assimilation of surrounding lithologies.

The correlations defined by our dataset in the Sr–Nd–Pb isotopic diagrams (cf. Doucelance et al. (2003) and Figs. 5 and 6) are similar to those observed in previous studies of the Southern Islands (Gerlach et al., 1988; Davies et al., 1989; Kokfelt et al., 1998; Christensen et al., 2001). This feature strongly suggests that our isotopic dataset reflects similar mixtures of the same two end-members. The convergence of the Southern and Northern Island trends in the $^{208}\text{Pb}/^{204}\text{Pb}$ – $^{206}\text{Pb}/^{204}\text{Pb}$ and $^{87}\text{Sr}/^{86}\text{Sr}$ – $^{206}\text{Pb}/^{204}\text{Pb}$ isotopic diagrams toward high $^{206}\text{Pb}/^{204}\text{Pb}$ values have led to the identification of a common moderate HIMU end-member ($^{206}\text{Pb}/^{204}\text{Pb}\sim 20$, cf. Gerlach et al. (1988); Hoernle et al. (2002); Doucelance et al. (2003)) and two others: (a) an EM1-like end-member for the Southern Islands; (b) the local depleted mantle for the Northern Islands. On the basis of all the isotopic diagrams, the two end-members are identified in the Os isotopic diagrams. Using the

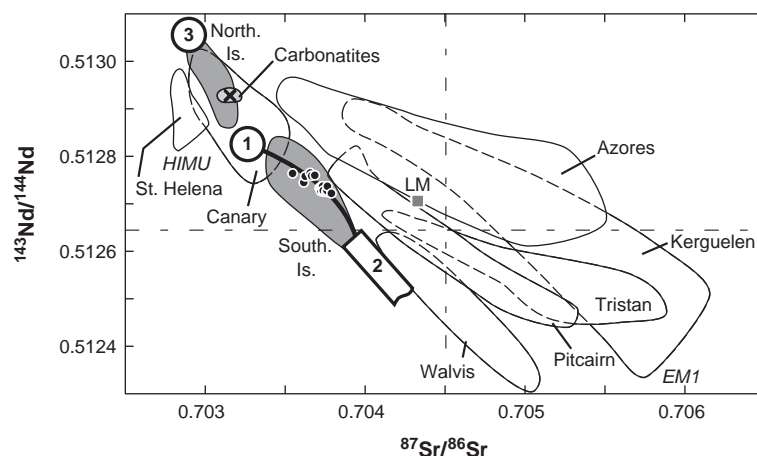


Fig. 5. $^{143}\text{Nd}/^{144}\text{Nd}$ vs. $^{87}\text{Sr}/^{86}\text{Sr}$ diagram for Cape Verde samples. Symbols correspond to Fogo samples which were analysed for Os: Circles=basalts; crosses=carbonatites. Grey fields=data from the Northern (Santo Antão, São Vicente, cf. Gerlach et al. (1988) and Southern Islands (Fogo: this study; Santiago: Gerlach et al. (1988)); Fogo carbonatites: this study and Hoernle et al. (2002). As basalts from Santiago show covariations between age and isotopic signature (Gerlach et al., 1988), only the latest volcanic series (Pico da Antonia formation) is plotted. The three Cape Verde end-members (see text for details) have the following compositions: for the common moderate HIMU end-member noted “1”: $^{143}\text{Nd}/^{144}\text{Nd}=0.51281$ and $^{87}\text{Sr}/^{86}\text{Sr}=0.70334$; for the enriched end-member of the Southern Islands noted “2”: $^{143}\text{Nd}/^{144}\text{Nd}=0.51262$ and $^{87}\text{Sr}/^{86}\text{Sr}=0.7040$; for the local depleted mantle end-member noted “3”: $^{143}\text{Nd}/^{144}\text{Nd}=0.51305$ and $^{87}\text{Sr}/^{86}\text{Sr}=0.7028$. The mixing hyperbola is calculated using the following concentration ratios: $(\text{Sr})_1/(\text{Sr})_2=3.3$ and $(\text{Nd})_1/(\text{Nd})_2=3$. For comparison we report fields for Walvis ridge basalts (Richardson et al., 1982) and the following Atlantic islands: St. Helena (Chaffey et al., 1989), Azores (Widom and Shirey, 1996), Canary (Hoernle et al., 1991; Marcantonio et al., 1995) and Tristan da Cunha (White and Hofmann, 1982; Le Roex et al., 1990; Cliff et al., 1991). Samples from the Southern and Northern Islands define two distinct domains. The Northern Islands define a steep trend with low $^{87}\text{Sr}/^{86}\text{Sr}$ and radiogenic $^{143}\text{Nd}/^{144}\text{Nd}$, almost parallel to the trend defined by St. Helena basalts. In contrast, the Southern Islands define a trend significantly steeper than the classical mantle array from the lowest $^{143}\text{Nd}/^{144}\text{Nd}$ value of the Northern Islands toward unradiogenic $^{143}\text{Nd}/^{144}\text{Nd}$ and moderately radiogenic $^{87}\text{Sr}/^{86}\text{Sr}$ ratios. Also reported are fields for Pitcairn for which the EMI-like signature has been explained by sediment contribution in the source (Woodhead and Devey, 1993; Eisele et al., 2002) and Kerguelen islands (Dosso and Murthy, 1980; White and Hofmann, 1982; Weis et al., 1993). HIMU is for the extreme HIMU end-member; EM1 corresponds to the Enriched Mantle 1 (Zindler and Hart, 1986). LM=Lower Mantle. Its isotopic composition ($^{87}\text{Sr}/^{86}\text{Sr}=0.70429$ and $^{143}\text{Nd}/^{144}\text{Nd}=0.51272$) is calculated as resulting from the mixture of Bulk Silicate Earth material and ~17% of Depleted Mantle (See Doucelance et al. (2003) for details).

converging isotopic trends defined by the Southern and Northern Islands, the composition of the moderate HIMU end-member is estimated: $^{187}\text{Os}/^{188}\text{Os}\sim 0.1325$, $^{206}\text{Pb}/^{204}\text{Pb}\sim 19.76$, $^{87}\text{Sr}/^{86}\text{Sr}\sim 0.70334$ and $^{143}\text{Nd}/^{144}\text{Nd}\sim 0.51281$. The location of the EM1-like end-member in the isotopic diagrams is less constrained. However, using the isotopic correlations, a possible isotopic composition can be estimated: $^{206}\text{Pb}/^{204}\text{Pb}\sim 18.60$, $^{87}\text{Sr}/^{86}\text{Sr}\sim 0.7040$ and $^{143}\text{Nd}/^{144}\text{Nd}\sim 0.51262$ and $^{187}\text{Os}/^{188}\text{Os}\sim 0.1450$. This composition has been chosen to plot at the enriched extremity of the Southern Island field in the different isotopic diagrams and one should keep in mind during the following discussion that the actual composition of the enriched component is likely to be more extreme.

5.3. Nature of the enriched end-member

On the basis of trace elements and Sr–Nd–Pb compositions, previous studies have identified the EM1-like end-member of Southern Islands as the sub-continental lithospheric mantle (SCLM) (Gerlach et al., 1988; Davies et al., 1989; Kokfelt et al., 1998; Doucelance et al., 2003). It should be noted that evidence has also been shown that fragments of continental lithosphere may be located beneath the eastern Canary Islands (Hoernle et al., 1991; Hoernle, 1998; Widom et al., 1999). The radiogenic Os isotopic composition we determine for the enriched end-member is an unexpected feature for the sub-continental lithospheric mantle. Indeed, most of the ultramafic xenoliths sampling SCLM display partic-

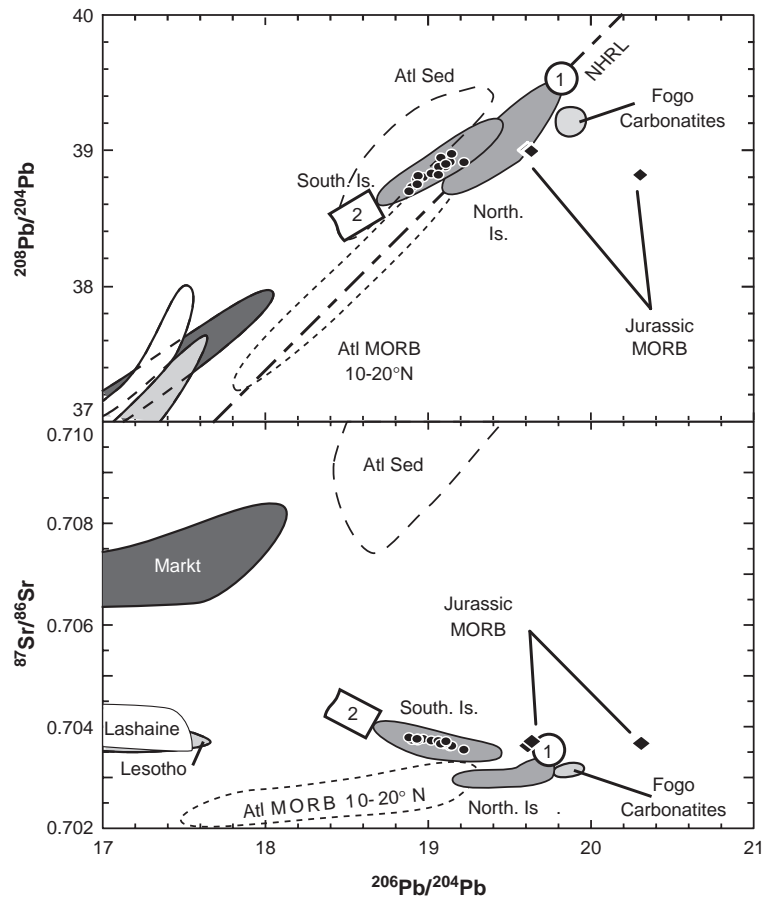


Fig. 6. $^{87}\text{Sr}/^{86}\text{Sr}$ and $^{208}\text{Pb}/^{204}\text{Pb}$ vs. $^{206}\text{Pb}/^{204}\text{Pb}$ diagram with potential candidates for the EM1-like end-member. Black circles correspond to Fogo samples analysed for Os. Black diamonds represent the local Jurassic MORB (Gerlach et al., 1988). Northern Islands (Santo Antão, São Vicente, cf. Gerlach et al. (1988)), Southern Islands (Fogo: this study; Santiago: Gerlach et al. (1988) and Fogo carbonatites (this study and Hoernle et al. (2002)) are reported as grey fields. The moderate HIMU and the EM1-like end-member compositions are plotted and labelled 1 and 2, respectively. The dashed fields are Atlantic sediments (White and Dupré, 1986; Hoernle et al., 1991; Hoernle, 1998) and the 10–20° N Atlantic MORB (Dosso et al., 1993). The dashed thick line represents the Northern Hemisphere Reference Line (Hart, 1984). Fields for the African lower continental crust (granulites from Lashaine, Lesotho and Markt groups (Rogers and Hawkesworth, 1982; Cohen et al., 1984; Huang et al., 1995) are also shown.

ularly unradiogenic $^{187}\text{Os}/^{188}\text{Os}$ ratios (average $^{187}\text{Os}/^{188}\text{Os} \approx 0.1214 \pm 0.0078$ (1σ)) (Walker et al., 1989; Carlson and Irving, 1994; Pearson et al., 1995; Chesley et al., 1999; Meisel et al., 2001; Schmidt and Snow, 2002). These low $^{187}\text{Os}/^{188}\text{Os}$ ratios reflect the evolution of a mantle reservoir with a low Re/Os due to the Re depletion associated with the crust extraction (Walker et al., 1989; Pearson et al., 1995). Even if some minerals have high Re/Os ratios and have developed radiogenic $^{187}\text{Os}/^{188}\text{Os}$ ratios with time, sulphides with low Re/Os dominate the Os budget of

ultramafic xenoliths and impose an unradiogenic bulk composition (Burton et al., 1999; Burton et al., 2000). The $^{187}\text{Os}/^{188}\text{Os}$ ratios measured in ultramafic xenoliths remain less radiogenic than those measured in Cape Verde basalts and the value estimated for the enriched end-member.

The contribution of the enriched end-member may be related to different processes occurring at different steps of the magma evolution, such as (1) the mixture with oceanic lithosphere melted by the thermal effect associated with the mantle plume, (2) the assimilation

in a magmatic chamber of the surrounding rocks or (3) the interaction with the oceanic crust during the magma ascent. In the following section, we investigate the different possible contaminants that may interact with the magma, with the aim of explaining the radiogenic Os isotopic compositions of basalts. This contaminant must account for Pb–Sr–Nd isotopic and trace elements compositions that have previously led to propose it to be the sub-continental lithospheric mantle, i.e. the steep trend defined by the Cape Verde Southern Islands in the Sr–Nd isotopic diagram which differs from those defined by other oceanic islands (Fig. 5) and the elevated $^{208}\text{Pb}/^{204}\text{Pb}$ and $^{207}\text{Pb}/^{204}\text{Pb}$ ratios for a given $^{206}\text{Pb}/^{204}\text{Pb}$.

5.3.1. Interaction with the volcanic pile

On the basis of our sampling, the assimilation of ancient lavas forming the volcanic pile during the latest stage of the magma ascent or interaction with the underlying lava flows can be rejected. Indeed, the temporal isotopic variation shows that the younger the lavas are, the more they have an EM1-like signature, with higher $^{87}\text{Sr}/^{86}\text{Sr}$ and $^{187}\text{Os}/^{188}\text{Os}$ and lower $^{206}\text{Pb}/^{204}\text{Pb}$ ratios. Conversely, the oldest lavas display isotopic compositions closer to the moderate HIMU end-member and cannot account for the EM1-like contaminant. Invoking older lavas that may not be sampled in this study, located deeper in the edifice, does not provide a more satisfying explanation. While these lavas could have high $^{87}\text{Sr}/^{86}\text{Sr}$ and $^{187}\text{Os}/^{188}\text{Os}$ ratios produced by post-eruption decay, the low $^{206}\text{Pb}/^{204}\text{Pb}$ ratio of the EM1-like end-member, lower than the moderate HIMU end-member composition, could not be explained. The enriched signature has to be related to an end-member that has undergone an evolution with a low U/Pb ratio. Thus, the variation of the Os, Sr, Nd and Pb isotopic ratios is related to the assimilation of deeper material.

5.3.2. Assimilation of oceanic crust or sediment

For most of the Os analyses of OIB (Marcantonio et al., 1995; Widom and Shirey, 1996; Widom et al., 1999), samples with concentrations lower than 30 ppt display a large range of Os isotopic ratios, up to 0.195, which is interpreted as sediment or crustal material assimilation during the magma ascent. Concerning Fogo basalts, neither Jurassic MORB identified by Gerlach et al. (1988) on the Southern Islands

nor actual Atlantic sediments can account for the end-member which displays $^{187}\text{Os}/^{188}\text{Os} \sim 0.1450$, $^{206}\text{Pb}/^{204}\text{Pb} \sim 18.60$, $^{87}\text{Sr}/^{86}\text{Sr} \sim 0.7040$ and $^{143}\text{Nd}/^{144}\text{Nd} \sim 0.51262$ (see Fig. 6). Jurassic MORB have the following isotopic compositions: $^{87}\text{Sr}/^{86}\text{Sr} = 0.703627 - 0.703707$, $^{143}\text{Nd}/^{144}\text{Nd} = 0.51306 - 0.51309$ and $^{206}\text{Pb}/^{204}\text{Pb} = 19.61 - 20.30$; they are not consistent with the EM1-like end-member identified in the Southern Islands. Despite the fact that Atlantic sediments (White and Dupré, 1986; Hoernle et al., 1991; Hoernle, 1998) with the lowest $^{206}\text{Pb}/^{204}\text{Pb}$ ratios possess Pb isotopic compositions that can account for the EM1-like end-member, they have $^{87}\text{Sr}/^{86}\text{Sr}$ ratios that are too radiogenic, which precludes them to be the contaminant.

5.3.3. Contribution of the underlying mantle

The contribution of the depleted MORB mantle has been already proposed (Gerlach et al., 1988; Davies et al., 1989; Doucelance et al., 2003) to explain the isotopic variation of the Northern Island basalts. As shown in Fig. 6, the field of the 10–20° N Atlantic MORB (Dosso et al., 1993) plots in the continuity of the Northern Island trend. This is not the case for the Southern Islands, which precludes a similar contribution in the source of Fogo. Moreover, the fact that assimilation of depleted mantle by oceanic basalts leads to unradiogenic Os isotopic ratios and an increase of Os content (Widom et al., 1999) also argues against such a contribution.

The carbonatites found on the Cape Verde Islands provide evidence that metasomatic processes occur in the underlying mantle. The carbonatites analyzed preserve radiogenic $^{187}\text{Os}/^{188}\text{Os}$ ratios consistent with the enriched end-member but too elevated in Pb and too low in Sr isotopic ratios (Fig. 6). In addition, Fogo basalts do not display high CaO contents compared to Northern Island basalts, as would be expected with a carbonatitic contribution. Generally, the low $^{143}\text{Nd}/^{144}\text{Nd}$ together with moderate $^{87}\text{Sr}/^{86}\text{Sr}$ measured in oceanic island basalts are attributed to a mantle metasomatized by migration of small volume of partial melt (Hawkesworth et al., 1984). Since the local Jurassic MORB have depleted compositions (Gerlach et al., 1988), the convecting mantle that formed the oceanic lithosphere consisted of depleted MORB mantle. Subsequent metasomatism of the oceanic lithospheric mantle

cannot explain the low $^{143}\text{Nd}/^{144}\text{Nd}$ ratios of Southern Island basalts which require a long evolution with a low Sm/Nd ratio. The end-member responsible for the enriched signature of Southern Island lavas must thus be related to an ancient material located in the oceanic lithosphere.

5.3.4. *Fragments of continental lithosphere within the oceanic lithosphere*

As developed above, the trace element and Pb–Sr isotopic compositions of the Southern Island basalts are consistent with sub-continental lithospheric mantle as the origin of the enriched signature (Gerlach et al., 1988; Davies et al., 1989; Kokfelt et al., 1998; Doucelance et al., 2003) but the radiogenic $^{187}\text{Os}/^{188}\text{Os}$ ratios measured in Fogo lavas require a high Re/Os component that cannot be the sub-continental lithospheric mantle. In earlier works, lower continental crust has been proposed to explain the enriched compositions of the Cape Verde and Canary volcanic rocks (Hoernle et al., 1991; Hoernle, 1998; Hoernle et al., 2002). From an Os isotopic point of view, xenoliths sampling the lower continental crust have radiogenic isotopic ratios ranging from 0.179 to 1.814 (Esperança et al., 1997; Saal et al., 1998) and highly variable Sr–Nd–Pb isotopic compositions related to the age of their formation and of the following events of metamorphism (Rudnick, 1992). In a recent study, Jull and Kelemen (2001) have shown that lower crust delamination may occur in several geological settings such as arcs, volcanic rifted margins and continental areas that are undergoing extension or removal of the underlying upper mantle. The extension associated with the opening of the Atlantic Ocean represents a favourable setting for lower crustal delamination and the location of the Cape Verde plateau, close to the African continent, suggests that some lower continental fragments could have been stored into the oceanic lithosphere. The presence of continental crust fragments found by drilling in the Iberian abyssal plain (Whitmarsh et al., 1998) supports such an assumption.

The fact that our estimate of the enriched end-member Os isotopic composition ($^{187}\text{Os}/^{188}\text{Os} \sim 0.1450$) does not fall within the lower continental crust range of compositions suggests that it has a more extreme location in the isotopic diagrams, with higher $^{187}\text{Os}/^{188}\text{Os}$, $^{87}\text{Sr}/^{86}\text{Sr}$ ratios and lower

$^{206}\text{Pb}/^{204}\text{Pb}$ and $^{143}\text{Nd}/^{144}\text{Nd}$ ratios. It should also be noted that, due to their low buoyancy, the upper lithospheric mantle and the lower part of the continental crust appears to be the most likely parts of the continental lithosphere to be delaminated (Kay and Mahlburg Kay, 1993). Because of the high contrast in Os content and Os isotopic ratios between the lower continental crust and the SCLM, a small amount of SCLM will significantly decrease the Os isotopic composition of the contaminant as well as increase its Os content. Thus, even a $^{187}\text{Os}/^{188}\text{Os}$ ratio close to 0.145 for the enriched contaminant would still be consistent with the lower continental crust if mixed with sub-continental lithospheric mantle.

The isotopic data available on the African granulites (Rogers and Hawkesworth, 1982; Cohen et al., 1984; Huang et al., 1995) show low $^{206}\text{Pb}/^{204}\text{Pb}$ ratios and unradiogenic $^{143}\text{Nd}/^{144}\text{Nd}$ associated with moderate $^{87}\text{Sr}/^{86}\text{Sr}$. In particular, the Markt group of granulite xenoliths from the margin of the Kaapvaal Craton have Sr–Nd–Pb isotopic compositions in good agreement with the correlations defined by our dataset (Fig. 6).

Incompatible trace element ratios also provide arguments in favour of the involvement of lower continental crust in the source of the Southern Islands. In a La/Ba vs. Nb/Ba plot (Fig. 7) the Southern and Northern Islands define two contiguous but distinct fields. Basalts from the Northern Islands define a trend toward high Nb/Ba and La/Ba values, consistent with a Depleted Mantle contribution. In contrast, the Southern Islands have lower La/Ba and Nb/Ba ratios and plot below the trend toward bulk continental crust values (Rudnick and Fountain, 1995) defined by the EM1-like basalts from the Atlantic Ocean (Humphris and Thompson, 1983; Le Roex, 1985; Weaver et al., 1987; Le Roex et al., 1990; Cliff et al., 1991) and from Pitcairn (Woodhead and Devey, 1993). The lack of correlation between trace element and isotopic ratios is related to the fact that our samples are derived from different parental magmas which have different fractionation and contamination histories. However, the Southern Islands trace element ratios support the involvement of a Ba-rich source in the Southern Islands, closer in composition to the granulites than to the bulk continental

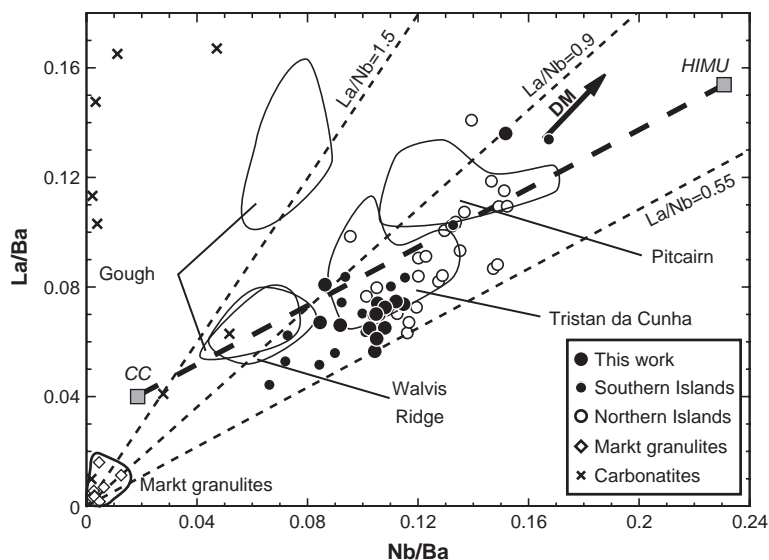


Fig. 7. La/Ba vs. Nb/Ba for Fogo basalts and samples from the whole archipelago with similar major element characteristics, Markt granulites (Huang et al., 1995) and Fogo carbonatites (Hoernle et al., 2002). CC=Continental Crust from (Rudnick and Fountain, 1995). The thick dashed line represents the mixture between (1) a continental crust-derived sediment with an average crustal composition and (2) the extreme HIMU end-member (Weaver, 1991). For comparison, we also show fields for Gough Island (Le Roex, 1985; Weaver et al., 1987), Walvis ridge basalts (Humphris and Thompson, 1983), Tristan da Cunha (Le Roex et al., 1990; Cliff et al., 1991) and Pitcairn Islands (Woodhead and Devey, 1993; Eisele et al., 2002). Cape Verde Southern Island basalts have a low Nb/La ratio and define a rough trend toward granulite-like compositions while the other oceanic basalts reported trend toward the CC composition.

crust composition, more representative of sediment compositions.

The temporal isotopic evolution of Fogo and Santiago basalts shows that the enriched end-member contribution increases through time (this study and Gerlach et al. (1988)). This temporal evolution supports that the lower crust fragments are located at shallow depth in the oceanic lithosphere. The mafic compositions of Fogo lavas imply that the lower crustal material is totally assimilated by the magma or at least melts to a high degree. Combining all these features suggests that the enriched signature of the Cape Verde Southern Island basalts is produced by interaction of the magma with lower continental crust fragments present at shallow depth in the oceanic lithosphere, possibly within the crust. The location of the enriched end-member is consistent with the conclusions of previous studies of Canary and Cape Verde Islands, for which the presence of fragments of continental lithosphere within the oceanic lithosphere was proposed (Gerlach et al., 1988; Davies et al., 1989; Hoernle et al., 1991; Hoernle, 1998; Widom et al., 1999).

5.4. Nature of the moderate HIMU end-member

Previous studies have proposed various origins for the moderate HIMU-like signature (Gerlach et al., 1988; Davies et al., 1989; Kokfelt et al., 1998; Christensen et al., 2001; Doucelance et al., 2003). Gerlach et al. (1988) and Davies et al. (1989) have proposed two different models involving, for the Southern Islands, a mixture between a DMM-HIMU hybrid end-member and an EM1-like end-member. Both their models are based on an ancient recycled oceanic crust (ROC) present either as a major component in the ascending plume or as an ubiquitous small-scale heterogeneity in the depleted mantle. Kokfelt et al. (1998) and Christensen et al. (2001) have suggested alternative models based on a so-called “young HIMU”, having a HIMU-like trace element pattern but moderate Pb isotopic ratios. Kokfelt et al. (1998) proposed this end-member to be associated with carbonatitic fluids produced during metasomatic processes while Christensen et al. (2001) argued in favour of “young” recycled oceanic crust (age not given). Recently, Doucelance et al.

(2003) have shown that a “young HIMU” cannot explain the most radiogenic Pb compositions of the Northern Islands. Using the helium evidence for lower mantle involvement (Christensen et al., 2001; Doucelance et al., 2003), they model the Sr and Pb isotopic composition of the moderate HIMU end-member as a mixture of lower mantle material and 1.6 Ga recycled oceanic crust.

The Os isotopic composition of the moderate HIMU end-member is the less radiogenic of the two Fogo end-members, significantly lower than the extreme HIMU-like signature ($^{187}\text{Os}/^{188}\text{Os} \sim 0.155$) defined by samples from the Austral-Cook Islands (Hauri and Hart, 1993; Reisberg et al., 1993; Schiano et al., 2001) or than the St. Helena values (~ 0.145) (Reisberg et al., 1993). We will show that such an unradiogenic value is fully consistent with a mixture of lower mantle material and a 1.6 Ga recycled oceanic crust as it has been proposed on the basis of Pb–Sr–He isotopes. Using the correlations that are observed in the isotopic diagrams, we will also

confirm that the HIMU-like end-member is not related to carbonatitic fluids.

5.4.1. Rejecting carbonatites as the HIMU-like end-member

If carbonatites are a common feature on continents, they are rare on oceanic islands (Allègre et al., 1971). Their origin is still discussed and we want to focus on their possible influence in the source of basalts. Recently, assimilation of carbonatites by the lavas has been proposed to explain trace element enrichment in some basaltic rocks erupted on São Vicente (Northern Islands, cf. Jorgensen and Holm (2002)). The Sr, Nd, Pb isotopic compositions of the two carbonatites reported in this work are similar to those previously analyzed (Gerlach et al., 1988; Hoernle et al., 2002). The locations in the different isotopic diagrams (Figs. 5, 6 and 8), with radiogenic $^{187}\text{Os}/^{188}\text{Os}$ and $^{208}\text{Pb}/^{204}\text{Pb}$ ratios that are too low relative to $^{206}\text{Pb}/^{204}\text{Pb}$ ratios preclude carbonatites from being the moderate HIMU end-member of Fogo

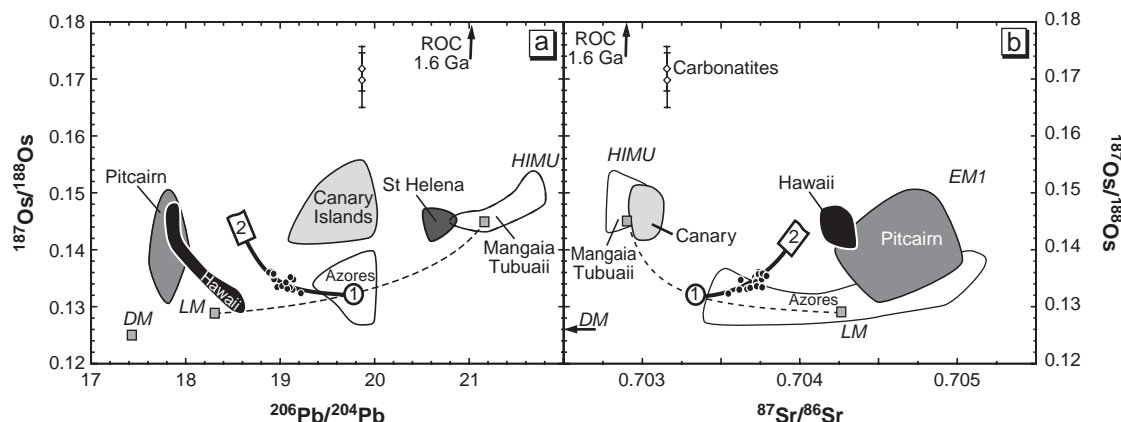


Fig. 8. (a) $^{187}\text{Os}/^{188}\text{Os}$ vs. $^{206}\text{Pb}/^{204}\text{Pb}$ and (b) $^{187}\text{Os}/^{188}\text{Os}$ vs. $^{87}\text{Sr}/^{86}\text{Sr}$ for Fogo samples. Black circles=basalts; open diamonds=carbonatites. LM=Lower Mantle; DM=Depleted Mantle; ROC=Recycled Oceanic Crust. HIMU is for the extreme HIMU end-member; EM1 corresponds to the Enriched Mantle 1 (Hauri and Hart, 1993; Reisberg et al., 1993). Also reported are fields for St. Helena (Reisberg et al., 1993); Azores (Widom and Shirey, 1996); Canary Islands (with Os>45 ppt from Marcantonio et al. (1995) and those from Widom et al. (1999) thought to be representative of the plume); Hawaii (Hauri et al., 1996); Mangaia, Tubuaiti (Hauri and Hart, 1993) and Pitcairn islands (Eisele et al., 2002). In comparison with the Azores and Canary Islands, Fogo lavas show less dispersion of the $^{187}\text{Os}/^{188}\text{Os}$ ratio relative to $^{206}\text{Pb}/^{204}\text{Pb}$ or $^{87}\text{Sr}/^{86}\text{Sr}$. This homogeneity does not reflect a sampling bias at the island scale since pre- and post-caldera samples have been analyzed. The $^{187}\text{Os}/^{188}\text{Os}$ variation is thought to reflect mixing effects. The locations of end-members “1” and “2” as well as concentration ratios used to calculate the mixing hyperbolas (plain curves) are computed to provide the best fit curves in the whole dataset. End-member “1”: $^{187}\text{Os}/^{188}\text{Os}=0.1325$, $^{87}\text{Sr}/^{86}\text{Sr}=0.70334$, $^{206}\text{Pb}/^{204}\text{Pb}=19.76$; End-member “2”: $^{187}\text{Os}/^{188}\text{Os}=0.1450$, $^{87}\text{Sr}/^{86}\text{Sr}=0.7040$, $^{206}\text{Pb}/^{204}\text{Pb}=18.60$; and $(\text{Sr})_1/(\text{Sr})_2=3.3$; $(\text{Pb})_1/(\text{Pb})_2=1$; $(\text{Os})_1/(\text{Os})_2=8.7$. The Os isotopic composition of 1.6 Ga recycled oceanic lithosphere is set at 0.145, by analogy with St. Helena and Mangaia basalts that have similar Pb isotopic compositions. Dashed curves represent mixing hyperbolas between this latter composition and that of the Lower Mantle (cf. Fig. 3 and Doucelance et al. (2003)). $(\text{Sr})_{\text{ROC}}/(\text{Sr})_{\text{LM}}=3$; $(\text{Pb})_{\text{ROC}}/(\text{Pb})_{\text{LM}}=1.33$; $(\text{Os})_{\text{ROC}}/(\text{Os})_{\text{LM}}=0.33$.

volcanism. The recent study of Cape Verde carbonatites by Hoernle et al. (2002) has shown that major and trace element as well as isotopic compositions of calcio-carbonatites located on Fogo, Brava, São Vicente and Santiago islands are consistent with metasomatic processes involving a low degree of melting of a recycled carbonated oceanic crust (1.6 Ga). However, the comparison of carbonatites and basalts from São Vicente has shown evidence of two separate HIMU sources located within the Cape Verde plume (Jorgensen and Holm, 2002). The high $^{187}\text{Os}/^{188}\text{Os}$ (up to 0.171) measured in carbonatites together with their Pb isotopic compositions are consistent with a HIMU source with high Re/Os for carbonatitic fluids distinct from the HIMU basaltic source and derived from 1.6 Ga ROC.

5.4.2. Recycled oceanic crust and lower mantle material

The presence of lower mantle material in the Cape Verde is supported by the high $^3\text{He}/^4\text{He}$ ratios measured in the Northern Island basalts by Christensen et al. (2001) and Doucelance et al. (2003). Despite the fact that Southern Island basalts tend toward the Cape Verde mantle plume composition in the Os–Pb–Sr–Nd isotopic diagrams, they do not display high $^3\text{He}/^4\text{He}$ ratios. This feature can be explained by the contribution of lower crustal material, which has low $^3\text{He}/^4\text{He}$, compensating for the primitive He signature.

The presence of lower mantle associated with recycled oceanic crust in the mantle plume is responsible for the unradiogenic Os isotopic composition of the moderate HIMU end-member, closer to the peridotitic mantle value (Roy-Barman and Allègre, 1994; Snow and Reisberg, 1995) than the extreme HIMU value (Hauri and Hart, 1993; Reisberg et al., 1993; Schiano et al., 2001). The lower mantle composition is thought to reflect the mixing of Bulk Silicate Earth material and depleted mantle in the proportion of 83:17 (Allègre and Lewin, 1989; Doucelance et al., 2003). The $^{187}\text{Os}/^{188}\text{Os}$ ratio of BSE (i.e. primitive mantle) has been estimated to $^{187}\text{Os}/^{188}\text{Os} \sim 0.1296 \pm 0.0008$ (Meisel et al., 2001), in good agreement with the chondrite compositions (Luck et al., 1980). Combined with the estimate of depleted mantle composition ($^{187}\text{Os}/^{188}\text{Os} \sim 0.125$) based on abyssal peridotites (Roy-Barman and Allègre, 1994; Snow and Reisberg, 1995), this yields a $^{187}\text{Os}/^{188}\text{Os}$

ratio close to 0.129 for the lower mantle, similar within the uncertainty to the BSE composition.

Estimating the Os isotopic evolution of recycled oceanic lithosphere remains a difficult task since it is composed of different layers (basalt, gabbro and depleted peridotite) with different Re/Os ratios and Os isotopic evolutions through time. Moreover the effects of melting and dehydration during subduction processes on the Re/Os ratios are not well enough constrained to enable precise and relevant calculations (Becker, 2000). Using an Os-evolution model of basalt with a low $^{187}\text{Re}/^{188}\text{Os}$ value of 50 (Widom et al., 1999) yields very radiogenic $^{187}\text{Os}/^{188}\text{Os}$ ratio of ~ 1.4 for 1.6 Ga recycled oceanic crust much more radiogenic than the extreme HIMU end-member. Hauri and Hart (1993) proposed the HIMU end-member corresponds to a mixture of recycled oceanic crust and mantle peridotite. The oceanic lithospheric mantle, which has a low $^{187}\text{Re}/^{188}\text{Os}$ ratio and a high Os content, would then lower the bulk $^{187}\text{Os}/^{188}\text{Os}$ of the recycled material. Due to the difference of Pb, Sr and Nd concentrations between oceanic crust and oceanic lithosphere peridotite, the latter would have a negligible effect on the Pb, Sr and Nd isotopic compositions.

In the case of the Cape Verde Islands, a 1.6 Ga recycled oceanic crust is associated with lower mantle material in the plume. Since the moderate HIMU end-member composition appears to be mainly dominated by the lower mantle material with high Os content and unradiogenic $^{187}\text{Os}/^{188}\text{Os}$ ratio, the Cape Verde lavas do not provide constraints on the composition of the 1.6 Ga recycled oceanic crust. However, by analogy with basalts from St. Helena (Reisberg et al., 1993) and Mangaia (Hauri and Hart, 1993; Schiano et al., 2001) with Pb isotopic compositions close to those calculated for a 1.6 Ga recycled oceanic crust, we estimate a $^{187}\text{Os}/^{188}\text{Os}$ ratio of 0.145 for the 1.6 Ga ROC melt-derived (Fig. 8). The mixture of such a component (1.6 Ga recycled oceanic crust and its residual mantle) with lower mantle material, illustrated in Fig. 8, reproduces the Os isotopic composition of the moderate HIMU end-member as proposed by Doucelance et al. (2003).

6. Conclusions

Our Os–Nd isotope dataset of Fogo lavas complements the work of Doucelance et al. (2003). The Sr–

Nd–Pb isotopic data show correlations similar to those previously observed between a moderate HIMU end-member and an EM1-like end-member. The correlations in the isotopic diagrams involving the Os and Nd isotopic ratios reflect the same mixing between the two end-members identified for the Southern Islands. The isotopic composition of the moderate HIMU end-member identified as the plume signature can be produced by the mixing of melts derived from 1.6 Ga recycled oceanic lithosphere and lower mantle material. The EM1-like end-member, previously identified as sub-continental lithospheric material on the basis of trace elements and Sr, Nd, Pb isotopic ratios, displays a radiogenic Os isotopic signature which requires the presence of a high Re/Os material. The temporal isotopic variation shows an increasing effect of the EM1-like end-member in the most recent lavas that supports the presence of the enriched end-member located at shallow depth in the oceanic lithosphere. The Os–Pb–Sr–Nd isotopic and trace element compositions of Fogo lavas lead to the identification of the contaminant as continental lithospheric fragments including lower continental crust, presently located under the Southern Islands and incorporated in the oceanic lithosphere during the Atlantic Ocean opening.

Acknowledgements

This work would not have gone so far without the stimulating discussions with A.E. Saal, C.H. Langmuir and A. Bezos. We thank L. Reisberg and E. Widom for their constructive and helpful reviews. P. Agrinier generously gave us the two carbonatites. RD work at GEOTOP was supported by a Lavoisier post-doctoral fellowship. This is IGP contribution 2034. [RLR]

References

- Allègre, C.J., Lewin, E., 1989. Chemical structure and history of the Earth: evidence from global non-linear inversion of isotopic data in a three-box model. *Earth Planet. Sci. Lett.* 96, 61–88.
- Allègre, C.J., Luck, J.-M., 1980. Osmium isotopes as petrogenetic and geological tracers. *Earth Planet. Sci. Lett.* 48, 148–154.
- Allègre, C.J., Turcotte, D.L., 1985. Geodynamical mixing in the mesosphere boundary layer and the origin of oceanic islands. *Geophys. Res. Lett.* 12, 207–210.
- Allègre, C.J., Pineau, F., Bernat, M., Javoy, M., 1971. Evidence for the occurrence of carbonatites on the Cape Verde and Canary islands. *Nature Phys. Sci.* 233, 103–104.
- Allègre, C.J., Hamelin, B., Provost, A., Dupré, B., 1986/87. Topology in isotopic multispace and origin of mantle chemical heterogeneities. *Earth Planet. Sci. Lett.*, 81, 319–337.
- Becker, H., 2000. Re–Os fractionation in eclogites and blueschists and the implications for recycling of oceanic crust into the mantle. *Earth Planet. Sci. Lett.* 177, 287–300.
- Bennet, V.C., East, T.M., Norman, M.D., 1996. Two mantle-plume components in Hawaiian picrites inferred from correlated Os–Pb isotopes. *Nature* 381, 221–224.
- Birck, J.-L., Roy-Barman, M., Capmas, F., 1997. Re–Os isotopic measurements at the femtomole level in natural samples. *Geostand. Newsl.* 20, 19–27.
- Brandon, A.D., Norman, M.D., Walker, R.J., Morgan, J.W., 1999. 1860s–1870s systematics of Hawaiian picrites. *Earth Planet. Sci. Lett.* 174, 25–42.
- Burton, K.W., Schiano, P., Birck, J.-L., Allègre, C.J., 1999. Osmium isotope disequilibrium between mantle minerals in a spinel-lherzolite. *Earth Planet. Sci. Lett.* 172, 311–322.
- Burton, K.W., et al., 2000. The distribution and behaviour of rhenium and osmium amongst mantle minerals and the age of the lithospheric mantle beneath Tanzania. *Earth Planet. Sci. Lett.* 183, 93–106.
- Burton, K.W., et al., 2002. The compatibility of rhenium and osmium in natural olivine and their behaviour during mantle melting and basalt genesis. *Earth Planet. Sci. Lett.* 198, 63–76.
- Carignan, J., Hild, P., Mevelle, G., Morel, J., Yeghichevan, D., 2001. Routine analyses of trace elements in geological samples using flow injection and low pressure on-line liquid chromatography coupled to ICP-MS: a study of reference materials BR, DR-N, UB-N, AN-G and GH. *Geostand. Newsl.* 25, 187–198.
- Carlson, R.W., Irving, A.J., 1994. Depletion and enrichment history of subcontinental lithospheric mantle; an Os, Sr, Nd and Pb isotopic study of ultramafic xenoliths from the northwestern Wyoming Craton. *Earth Planet. Sci. Lett.* 126, 457–472.
- Chaffey, D.J., Cliff, R.A., Wilson, B.M., 1989. Characterization of the St. Helena magma source. *Geol. Soc. London Spec. Publ.* 42, 257–276.
- Chauvel, C., Hofmann, A.W., Vidal, P., 1992. HIMU-EM: the French Polynesian connection. *Earth Planet. Sci. Lett.* 110, 99–119.
- Chesley, J.T., Rudnick, R.L., Lee, C.-T., 1999. Re–Os systematics of mantle xenoliths from the East African Rift: age, structure, and history of the Tanzanian craton. *Geochim. Cosmochim. Acta* 63 (7–8), 1203–1217.
- Christensen, B.P., Holm, P.M., Jambon, A., Wilson, J.R., 2001. Helium, argon and lead isotopic composition of volcanics from Santo Antão and Fogo, Cape Verde Islands. *Chem. Geol.* 178, 127–142.
- Cliff, R.A., Baker, P.E., Mather, N.J., 1991. Geochemistry of inaccessible island volcanics. *Chem. Geol.* 92, 251–260.
- Cohen, R.S., O’Nions, R.K., 1982. Identification of recycled continental material in the mantle from Sr, Nd and Pb isotope investigations. *Earth Planet. Sci. Lett.* 61, 73–84.

- Cohen, R.S., O'Nions, R.K., Dawson, J.B., 1984. Isotope geochemistry of xenoliths from East Africa: implications for development of mantle reservoirs and their interaction. *Earth Planet. Sci. Lett.* 68, 209–220.
- Davies, G.R., Norry, M.J., Gerlach, D.C., Cliff, R.A., 1989. A combined chemical and Pb–Sr–Nd isotope study of the Azores and Cape Verde hot-spots: the geodynamic implications, magmatism in the ocean basins. *Geol. Soc. Spec. Publ.* 42, 231–255.
- Day, S.J., Heleno da Silva, S.I.N., Fonseca, J.F.B.D., 1999. A past giant lateral collapse and present-day flank instability of Fogo, Cape Verde Islands. *J. Volcanol. Geotherm. Res.* 94, 191–218.
- Dosso, L., Murthy, V.R., 1980. A Nd isotopic study of the Kerguelen Islands; inferences on enriched oceanic mantle sources. *Earth Planet. Sci. Lett.* 48, 268–276.
- Dosso, L., Bougault, H., Joron, J.-L., 1993. Geochemical morphology of the North Mid-Atlantic Ridge, 10°–20° N: trace element-isotopic complementarity. *Earth Planet. Sci. Lett.* 120, 443–462.
- Doucelance, R., Escrig, S., Moreira, M., Gariépy, C., Kurz, M., 2003. Pb–Sr–He isotope and trace element geochemistry of the Cape Verde Archipelago. *Geochim. Cosmochim. Acta* 67 (19), 3717–3733.
- Eisele, J., et al., 2002. The role of sediment recycling in EM-1 inferred from Os, Pb, Hf, Nd, Sr isotope and trace element systematics of the Pitcairn hotspot. *Earth Planet. Sci. Lett.* 196, 197–212.
- Esperança, R.W., Carlson, R.W., Shirey, S.B., Smith, D., 1997. Dating crust-mantle separation: Re–Os isotopic study of mafic xenoliths from central Arizona. *Geology* 25, 651–654.
- Gerlach, D.C., Cliff, R.A., Davies, G.R., Norry, M.J., Hodgson, N., 1988. Magma sources of the Cape Verdes archipelago: isotopic and trace element constraints. *Geochim. Cosmochim. Acta* 52, 2979–2992.
- Hart, S.R., 1984. A large-scale isotope anomaly in the southern hemisphere mantle. *Nature* 309, 753–757.
- Hart, S.R., 1988. Heterogeneous mantle domains: signatures, genesis and mixing chronologies. *Earth Planet. Sci. Lett.* 90, 273–296.
- Hart, S.R., Davis, K.E., 1978. Nickel partitioning between olivine and silicate melt. *Earth Planet. Sci. Lett.* 40, 203–219.
- Hauri, E.H., Hart, S.R., 1993. Re–Os isotope systematics of HIMU and EMII oceanic island basalts from the south Pacific Ocean. *Earth Planet. Sci. Lett.* 114, 353–371.
- Hauri, E.H., Lassiter, J.C., DePaolo, D.J., 1996. Os isotope systematics of drilled lavas from Mauna Loa, Hawaii. *J. Geophys. Res.* 101, 11793–11806.
- Hawkesworth, C.J., Rogers, N.W., VanCalsteren, P.W., Menzies, M.A., 1984. Mantle enrichment processes. *Nature* 311, 331–335.
- Hawkesworth, C.J., Kempton, P.D., Rogers, N.W., Ellam, R.M., Van Calsteren, P.W., 1990. Continental mantle lithosphere and shallow level enrichment processes in the Earth's mantle. *Earth Planet. Sci. Lett.* 96, 256–268.
- Hodgson, N., 1986. Carbonatites and associated rocks from the Cape Verde islands. Unpublished thesis Thesis, University of Leicester.
- Hoernle, K., 1998. Geochemistry of Jurassic oceanic crust beneath Gran Canaria (Canary Islands): implications for crustal recycling and assimilation. *J. Petrol.* 39, 859–880.
- Hoernle, K., Tilton, G., Schmincke, H.-U., 1991. Sr–Nd–Pb isotopic evolution of Gran Canaria: evidence for shallow enriched mantle beneath the Canary Islands. *Earth Planet. Sci. Lett.* 106, 44–63.
- Hoernle, K., Tilton, G., Le Bas, M.J., Duggen, S., Garbe-Schönberg, D., 2002. Geochemistry of oceanic carbonatites compared with continental carbonatites: mantle recycling of oceanic crustal carbonate. *Contrib. Mineral. Petrol.* 142, 520–542.
- Huang, Y.-M., Van Calsteren, P.W., Hawkesworth, C.J., 1995. The evolution of the lithosphere in southern Africa: a perspective on the basic granulite xenoliths from kimberlites in south Africa. *Geochim. Cosmochim. Acta* 59, 4905–4920.
- Humphris, S.E., Thompson, G., 1983. Geochemistry of rare earth elements in basalts from the Walvis Ridge; implications for its origin and evolution. *Earth Planet. Sci. Lett.* 66, 223–242.
- Jorgensen, J.O., Holm, P.M., 2002. Temporal variation and carbonatite contamination in primitive ocean island volcanics from Sao Vicente, Cape Verde Islands. *Chem. Geol.* 195, 249–267.
- Jull, M., Kelemen, P.B., 2001. On the condition for lower crust convective instability. *J. Geophys. Res.* 106, 6423–6446.
- Kay, R.W., Mahlburg Kay, S., 1993. Delamination and delamination magmatism. *Tectonophysics* 219, 177–189.
- Kokfelt, T.F., Holm, P.M., Hawkesworth, C.J., Peate, D.W., 1998. A lithospheric mantle source for the Cape Verde Island magmatism: trace element and isotopic evidence from the island of Fogo. *Min. Mag.* 62A, 801–802.
- Kurz, M., Jenkins, W.J., Schilling, J.G., Hart, S.R., 1982. Helium isotopic systematics of ocean islands and mantle heterogeneity. *Nature* 297, 43–47.
- Lancelot, J.R., Allègre, C.J., 1974. Origin of carbonatitic magma in the light of the Pb–U–Th isotope system. *Earth Planet. Sci. Lett.* 22, 233–238.
- Lassiter, J.C., 2003. Rhenium volatility in subaerial lavas: constraints from subaerial and submarine portions of the HSDP-2 Mauna Kea drillcore. *Earth Planet. Sci. Lett.* 214, 311–325.
- Lassiter, J.C., Hauri, E.H., 1998. Osmium-isotope variations in Hawaiian lavas: evidence for recycled oceanic lithosphere in the Hawaiian plume. *Earth Planet. Sci. Lett.* 164, 483–496.
- Le Roex, A.P., 1985. Geochemistry, mineralogy, and magmatic evolution of the basaltic and trachytic lavas from Gough Island, South Atlantic. *J. Petrol.* 26, 149–186.
- Le Roex, A.P., Cliff, R., Adair, B., 1990. Tristan da Cunha, south Atlantic: geochemistry and petrogenesis of a basanite–phonolite lava series. *J. Petrol.* 31, 779–812.
- Luck, J.M., Birck, J.L., Allègre, C.J., 1980. 187Re–187Os systematics in meteorites: early chronology of the solar system and the age of the Galaxy. *Nature* 283, 256–259.
- Marcantonio, F., Zindler, A., Elliot, T., Staudigel, H., 1995. Os isotope systematics of La Palma, Canary islands: evidence for recycled crust in the mantle source of HIMU ocean islands. *Earth Planet. Sci. Lett.* 133, 397–410.

- Matos Alves, C.A., Macedo, J.R., Silva, L.C., Serralheiro, A., Peixoto, A.F., 1979. Estudo geológico, petrológico e vulcanológico da Ilha de Santiago (Cabo Verde). *Garcia de Orta, Sér. Geol. Lisboa* 3, 9–27.
- McKenzie, D., O’Nions, R.K., 1983. Mantle reservoirs and ocean island basalts. *Nature* 301, 229–231.
- Meisel, T., Walker, R.J., Morgan, J.W., 1996. The osmium isotopic composition of the Earth’s primitive upper mantle. *Nature* 383, 517–520.
- Meisel, T., Walker, R.J., Irving, A.J., J.-P., L., 2001. Osmium isotopic compositions of mantle xenoliths: a global perspective. *Geochim. Cosmochim. Acta* 65, 1311–1323.
- Pearson, D.G., Carlson, R.W., Shirey, S.B., Boyd, F.R., Nixon, P.H., 1995. Stabilisation of Archean lithospheric mantle: a Re–Os isotope study of peridotite xenoliths from the Kaapvaal craton. *Earth Planet. Sci. Lett.* 134, 341–357.
- Reisberg, L., et al., 1993. Os isotope systematics in ocean island basalts. *Earth Planet. Sci. Lett.* 120, 149–167.
- Richard, P., Shimizu, N., Allègre, C.J., 1976. $^{143}\text{Nd}/^{146}\text{Nd}$, a natural tracer: an application to oceanic basalts. *Earth Planet. Sci. Lett.* 31, 269–278.
- Richardson, S.H., Erlank, A.J., Duncan, A.R., Reid, D.L., 1982. Correlated Nd, Sr and Pb isotope variation in walvis ridge basalts and implications for evolution of their mantle source. *Earth Planet. Sci. Lett.* 59, 327–352.
- Rogers, N.W., Hawkesworth, C.J., 1982. Proterozoic age and cumulate origin for granulite xenoliths, Lesotho. *Nature* 299, 409–413.
- Roy-Barman, M., Allègre, C.J., 1994. $^{187}\text{Os}/^{186}\text{Os}$ ratios in mid-ocean ridge basalts and abyssal peridotites. *Geochim. Cosmochim. Acta* 58, 5043–5054.
- Roy-Barman, M., Allègre, C.J., 1995. $^{187}\text{Os}/^{186}\text{Os}$ in oceanic island basalt: tracing oceanic crust recycling in the mantle. *Earth Planet. Sci. Lett.* 129, 145–161.
- Rudnick, R.L., 1992. Samples of lower continental crust. In: Fountain, D.M., Arculus, R., Kay, R. (Eds.), *The Continental Lower Crust*. Elsevier, Amsterdam, pp. 269–316.
- Rudnick, R.L., Fountain, D.M., 1995. Nature and composition of the continental crust: a lower crustal perspective. *Rev. Geophys.* 33, 267–309.
- Saal, A.E., Rudnick, R.L., Ravizza, G.E., Hart, S.R., 1998. Re–Os isotope evidence for the composition, formation and age of the lower continental crust. *Nature* 393, 58–61.
- Schiano, P., Burton, K.W., Dupré, B., Brick, J.-L., Allègre, C.J., 2001. Correlated Os–Pb–Nd–Sr isotopes in the Austral-Cook chain basalts: the nature of mantle components in plume sources. *Earth Planet. Sci. Lett.* 186, 353–371.
- Schmidt, G., Snow, J.E., 2002. Os isotopes in mantle xenoliths from the Eifel volcanic field and the Vogelsberg (Germany): age constraints on the lithospheric mantle. *Contrib. Mineral. Petrol.* 143, 694–705.
- Smoliar, M.I., Walker, R.J., Morgan, J.W., 1996. Re–Os ages of group IIA, IIIA, IVA and IVB iron meteorites. *Science* 271, 1099–1102.
- Snow, J.E., Reisberg, L., 1995. Os isotopic systematics of the MORB mantle: results from altered abyssal peridotites. *Earth Planet. Sci. Lett.* 133, 411–421.
- Thirlwall, M.F., 1997. Pb isotopic and elemental evidence for OIB derivation from young HIMU mantle. *Chem. Geol.* 139, 51–74.
- Walker, R.J., Carlson, R.W., Shirey, S.B., Boyd, F.R., 1989. Os, Sr, Nd, and Pb isotope systematics of southern African peridotite xenoliths: implications for the chemical evolution of subcontinental mantle. *Geochim. Cosmochim. Acta* 53, 1583–1595.
- Walker, R.J., Hanski, E., Vuollo, J., Lippo, J., 1996. The Os isotopic composition of Proterozoic upper mantle; evidence for chondritic upper mantle from the Outokumpu Ophiolite, Finland. *Earth Planet. Sci. Lett.* 141, 161–173.
- Weaver, B., 1991. The origin of ocean island basalt end-member compositions: trace element and isotopic constraint. *Earth Planet. Sci. Lett.* 104, 381–397.
- Weaver, B.L., Wood, D.A., Tarney, J., Joron, J.-L., 1987. Geochemistry of ocean island basalts from the South Atlantic; Ascension, Bouvet, St. Helena, Gough and Tristan da Cunha. *Geol. Soc. London Spec. Publ.* 30, 253–267.
- Weis, D., Frey, F.A., Leyrit, H., Gautier, I., 1993. Kerguelen Archipelago revisited; geochemical and isotopic study of the Southeast Province lavas. *Earth Planet. Sci. Lett.* 118, 101–119.
- White, W.M., 1985. Sources of oceanic basalts: radiogenic isotope evidence. *Geology* 13, 115–118.
- White, W., Dupré, B., 1986. Sediment subduction and magma genesis in the Lesser Antilles; isotopic and trace element constraints. *J. Geophys. Res.* 91, 5927–5941.
- White, W.M., Hofmann, A.W., 1982. Sr and Nd isotope geochemistry of oceanic basalts and mantle evolution. *Nature* 296, 821–825.
- Whitmarsh, R.B., 1998. Drilling reveals transition from continental breakup to early magmatic crust. *EOS Trans. Am. Geophys. Union* 79 (14), 173–181.
- Widom, E., Shirey, S.B., 1996. Os isotope systematics in the Azores: implications for mantle plume sources. *Earth Planet. Sci. Lett.* 142, 451–465.
- Widom, E., Hoernle, K., Shirey, S.B., Schmincke, H.-U., 1999. Os isotope systematics in the Canary Islands and Madeira: lithospheric contamination and mantle plume signatures. *J. Petrol.* 40, 276–296.
- Woodhead, J.D., Devey, C.W., 1993. Geochemistry of the Pitcairn seamounts: I. Source character and temporal trends. *Earth Planet. Sci. Lett.* 116, 81–99.
- Zindler, A., Hart, S.R., 1986. Chemical geodynamics. *Ann. Rev. Earth Planet. Sci.* 14, 493–571.